Biogeosciences

Discussions

Open Access

Origin, transport, and retention of fluvial sedimentary organic matter in South Africa's largest freshwater wetland, Mkhuze Wetland System

Julia Gensel[1], Marc Steven Humphries[2], Matthias Zabel[1], David Sebag[3,4], Annette Hahn[1], and Enno Schefuß[1]

[1]MARUM - Center for Marine Environmental Sciences, University of Bremen, Bremen, Germany
[2]School of Chemistry, University of the Witwatersrand, Johannesburg, South Africa
[3]IFP Energies Nouvelles, Direction Sciences de la Terre et Technologies de l'Environnement, France
[4]Normandie Univ, UNIROUEN, UNICAEN, CNRS, M2C, 76000 Rouen, France

Correspondence: Julia Gensel (julia.gensel@mail.de)

Abstract. Sedimentary organic matter (OM) analyses along a 130 km-long transect of the Mkhuze River from the Lebombo Mountains to its outlet into Lake St. Lucia, Africa's most extensive estuarine system, revealed the present active trapping function of a terminal freshwater wetland. A combination of organic bulk parameters, thermal analyses, and determination of plant waxes, and their corresponding stable carbon (δ^{13}C) and hydrogen (δD) isotopic signatures in surface sediments and local

5   plant species enabled characterization and comparison of sedimentary OM in terms of stability, degradation status, sources, and sinks within and among the respective sub-environments of the Mkhuze Wetland System. This approach showed that fluvial sedimentary OM originating from inland areas is mainly deposited on the floodplain and Mkhuze Swamps. In contrast to samples from upstream areas, a distinctly less degraded signature characterizes the sedimentary OM in the northern section of Lake St. Lucia. Although lake sedimentary plant waxes are similar in the observed wax distribution pattern and δ^{13}C values,

10   they exhibit considerably higher δD values. This offset in δD indicates that lakeshore vegetation dominates plant-derived sedimentary OM in the lake, elucidating the effective capturing of OM and its fate in a sub-tropical coastal freshwater wetland. These findings raise important constraints for environmental studies assuming watershed-integrated signals in sedimentary archives retrieved from downstream lakes or offshore.

1   Introduction

15   Lake St. Lucia is the largest estuarine system in Africa and is of both local and international importance (Porter, 2013). It is a biodiversity hotspot and provides habitat for fish, wildlife, and breeding grounds for birds. On this basis, it significantly supports national and international ecotourism as well as the regional economy (Whitfield and Taylor, 2009). Its functioning is highly dependent on a constant supply of freshwater. One of the major hydrological inputs into Lake St. Lucia is the Mkhuze Wetland System, South Africa's largest freshwater wetland system, which accounts for about 56 % of the freshwater input to

20   the lake (Stormanns, 1987). It is part of the iSimangaliso Wetland Park, which was declared a UNESCO World Heritage Site in

1999 (Taylor et al., 2006), was designated a Ramsar site in 1986 (Perissinotto et al., 2013), and is the World's oldest formally protected estuary (Whitfield and Taylor, 2009).

Wetlands act as filters by removing or retaining nutrients and man-made pollutants (Reddy and Debusk, 1987). They also control sedimentation through deposition, resulting in less siltation in adjacent water systems (Johnston, 1991). When a wet-
25 land's natural filter function is overstressed, the wetland and its beneficial functions can be destroyed (Hemond and Benoit, 1988; Junk and An, 2013). In the worst case, the wetland can become a source of pollutants and sediments that have been previously filtered and stored. The Mkhuze Wetland System, and in particular the Mkhuze Swamps, are supposedly such a filter for Lake St. Lucia's water supply and therefore presumably provide the benefits mentioned above.

Like most wetlands, the Mkhuze Wetland System is affected by human interference. For instance, cattle grazing and use
30 as agricultural land are reported to be of increasing importance for both sugarcane and eucalyptus cultivation (Neal, 2001). Human activities such as channel dredging (Mpempe and Tshanetshe canals) have also significantly altered the natural state (Neal, 2001; Barnes et al., 2002; Ellery et al., 2003). Such disturbances have the potential to cause alteration of vegetation, hydrologic conditions, as well as sediment balance and transport pathways. Such negative impacts have extensively been studied for the swamp system formerly present to the south of Lake St. Lucia, the Mfolozi Swamps (Whitfield and Taylor,
35 2009; Taylor, 2013, and references therein).

Our study aims to assess the current status of the Mkhuze Wetland System located north of the lake, in particular the Mkhuze Swamps, and thereby to evaluate the current wetland's impact on Lake St. Lucia. We analyzed surface sediments along a 130 km-long transect from the Mkhuze River channel to its mouth in Lake St. Lucia, as well as extending into the northern part of Lake St. Lucia.

40 Analyses of vegetation biomarkers in these samples enable the identification of the dominant vegetation providing information about the hydrological conditions in the system, since indicative plant species grow only under certain hydrologic conditions. Based on the characteristic distribution patterns of n-alkanes originating from plant waxes, in combination with their respective stable carbon isotope signatures (Ficken et al., 2000; Rommerskirchen et al., 2006; Vogts et al., 2009; Diefendorf and Freimuth, 2017, and reference therein), we draw conclusions about the dominant vegetation types contributing to the
45 sedimentary OM. Analysis of compound specific hydrogen isotopes provides additional information about the hydrologic conditions (Sachse et al., 2012; Sessions, 2016, and references therein). Because plant waxes represent only a small fraction of the total sedimentary organic material, bulk organic characteristics are inferred from analyses of total organic carbon (TOC) and carbon to nitrogen ratios, as well as Rock-Eval® thermal analyses to determine bulk organic matter stability, degradation, and preservation status. Combining these approaches allows to characterize the deposited sedimentary organic material within each
50 sub-environment of the system and identify sources, sinks, and transport pathways of the organic material within the Mkhuze Wetland System. This enables us to assess the status of the wetland system in terms of its filter function and influence on Lake St. Lucia.

The filtering function of wetlands is of particular interest because wetlands are considered to be either sources or sinks of organic carbon and therefore may, among other things, increase carbon emissions from surface waters if they export organic
55 carbon (OC) in substantial amounts to adjacent water systems and vice versa (e.g, Cole et al., 2007; Reddy and DeLaune, 2008;
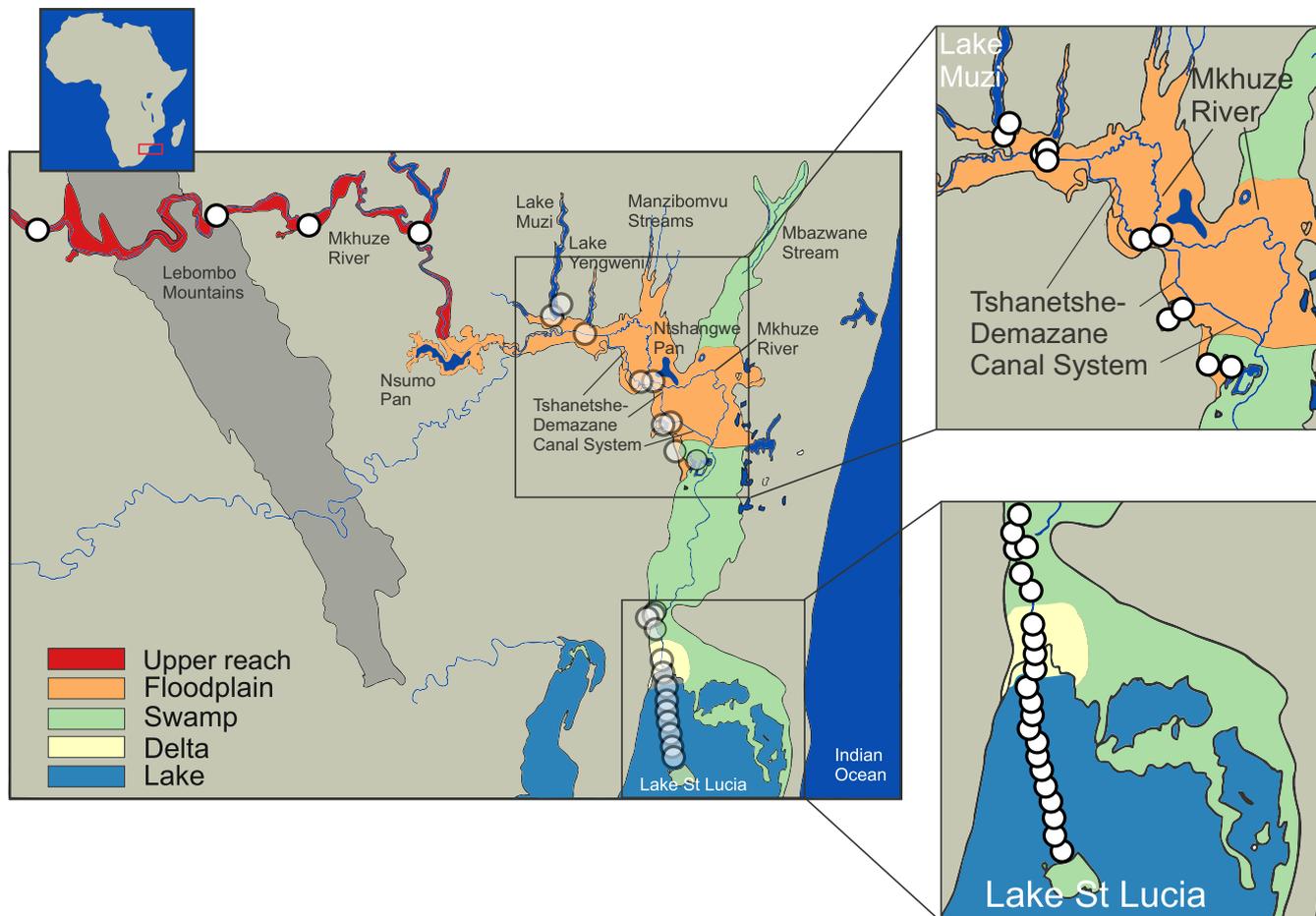
Figure 1. Map of the Mkhuze catchment area. White circles represent sampling locations and coloured areas refer to the assigned sub-environments. Important geologic features, including watercourses and major lakes or pans, are named.

Mitsch and Gosselink, 2015). The factors controlling whether a wetland serves as a source or sink are not yet fully understood, but it is undeniable that wetland hydrology always has a critical role in these processes. This study provides insights into the characteristics and transport of organic matter in a terminal wetland under subtropical climatic conditions. These characteristics which also can be identified in other wetlands around the World reveal potential implications for (paleo)environmental studies based on sedimentary archives from downstream areas.

2   Material and Methods

2.1   Study Site

The Mkhuze Wetland System (27.8° S, 32.5° E; Figure 1), South Africa's largest freshwater wetland system (~ 450 km^2), is located in the northeastern coastal region of South Africa in the KwaZulu-Natal province. It is bordered by the Lebombo
65   Mountain Range to the west and the Indian Ocean to the east, and forms a mosaic of wetland types, including swamp forests, grassy swamps, and open water (pans) (Stormanns, 1987). This ecological heterogeneity and biotic diversity are of international conservation importance, and therefore listed as a wetland of international importance by the RAMSAR Convention.

2.1.1   Hydrology, vegetation and depositional sub-environments.

Two major hydrologic inflows supply water to the Mkhuze Wetland System, the Mkhuze River and Manzimbomvu streams,
70   either through local runoff, direct precipitation, or groundwater inflow (Ellery et al., 2003).

The major tributary is the Mkhuze River, which originates east of Vryheid (~ 125 km inland) and drains a catchment area of about 5250 km^2 (see Figure 2) consisting mainly Cretaceous-Quaternary aged sedimentary cover of the coastal plain (McCarthy and Hancox, 2000). The river is fed primarily by direct precipitation and is characterized by a mean annual discharge of about 211 to 326 x 10^6 m^3 (Hutchison and Pitman, 1973). Water flow varies greatly seasonally and interannually, but is generally
75   highest during the austral summer months and lowest to nonexistent during the winter months (McCarthy and Hancox, 2000). The river drains sedimentary strata of the Dwyka, Ecca and lower Beaufort Groups (Karoo Supergroup), as well as Pongola granites and rhyolites in the Lebombo Mountains (McCarthy and Hancox, 2000). It transports comparatively high amounts of sediment dominated by fine, kaolinitic clays originating from Pongola granites and Karoo Supergroup sedimentary rocks (McCarthy and Hancox, 2000).

80   The second hydrologic input is water from the groundwater-fed streams from the north (Manzimbomvu Streams) (Stormanns, 1987; Barnes et al., 2002). Unlike discharge in the Mkhuze River, these streams are characterized by regular, persistent flow and transport negligible amounts of suspended sediment. The Mkhuze Wetland System can be divided into various sub-environments reflecting different depositional and geomorphological characteristics, namely the upper reach, the floodplain, the Mkhuze Swamps, and the outlet to Lake St. Lucia. The upper reach (Figure 1, reddish colour) is the section extending from
85   east of the Lebombo Mountain Range to the Nsumo Pan. It is dominated by trees, such as *Acacia xanthophloea* and *Ficus sycomorus* along the river course (Taylor, 1982b). The Mkhuze River in this area is a degrading river being largely confined to its channel (Alexander et al., 1986).

Farther downstream, the river traverses a sandy coastal plain where it forms an extensive floodplain (Figure 1, orange colour) which is characterized by a variety of vegetation communities (*Phragmites mauritianus* reed swamp community, *Imperata*
90   *cylindrica* hygrohilious grassland community, *Echinochloa pyramidalis* backswamp community, *Ficus sycomorus* riparian forest community distributed along the Mkhuze River, *Cynodon dactylon* floodplain community, *Acacia xanthophloea* woodland community, and the *Nymphaea sp* aquatic community; Tinley, 1959; Neal, 2001, Figure 3) and partly used for agricultural purposes. During periods of high flow, the Mkhuze River overtops its banks and inundates the floodplain (Alexander, 1973).

Flooding results in sediment deposition in the immediate vicinity of the channel due to slower flow velocity caused by ripar-
95 ian vegetation, resulting in the formation of natural levees (Stormanns, 1987; Neal, 2001; Ellery et al., 2011), as well as the
recharge of pans located in the north-south oriented fossil dune system. As a result, the Mkhuze River is a highly dynamic
and rapidly aggrading system, characterized by relatively high sedimentation rates (0.25 - 0.50 cm/yr; Humphries et al., 2010).
Loss of water to the surrounding floodplain results in marked reductions in downstream channel size and the Mkhuze River
gradually loses definition before terminating in a large freshwater swamp, termed the Mkhuze Swamps (Figure 1, greenish
100 colour). The Mkhuze Swamps function as an intermediate reservoir that fills with water during the summer and releases it
into Lake St. Lucia (Figure 1, bluish colour) from the beginning of the dry season when the lake is no longer primarily fed by
direct precipitation (Alexander, 1973; Taylor, 1982b). Dominant vegetation of the Mkhuze Swamps include *Cyperus papyrus*,
Phragmites mauritianus, and *Echinochloa pyramidalis* (Taylor, 1982b). On the levees *Ficus sycamorus* and *Ficus trichopoda*
occur, whereas the pans are characterized by *Nymphacaea sp* (Taylor, 1982b). In the northern parts of Lake St. Lucia nearly
105 monospecific stands of the salt-tolerant *Sporobolus virginicus* can be found (Stormanns, 1987). Because Lake St. Lucia is an
extremely shallow lake (average depth ~1 m), it is highly susceptible to evaporative losses (~1380 mm/year, Hutchison and
Pitman, 1973) and dependent on constant water supply from the swamp system.

2.1.2 Climate

The study area experiences a subtropical climate characterized by hot, humid summers and mild, dry winters and mean annual
110 temperatures ranging from 21 °C to 23 °C. The Mkhuze Wetland System lies within the summer rainfall zone of South Africa,
with about 60 % of precipitation occurring during the austral summer months (November through March) in association with
cold fronts moving northward along the coast. Precipitation gradually decreases from east to west (see Figure 2, Van Heerden
and Swart, 1986) from 1000 mm/year to 600 mm/year (Hutchison, 1976; Maud, 1980). Flooding is highly variable and usually
associated with cutoff low pressure systems that develop during December and January, or infrequent tropical cyclones. Evap-
115 otranspiration rates are considered relatively high, ranging from 80 mm per month in winter to 190 mm per month in summer
(Watkeys et al., 1993).

2.1.3 Man-made changes

The course of the Mkhuze River has been greatly altered by human intervention, beginning in the early 1970s. A prolonged
drought (1968 - 1971) resulted in hypersaline conditions in Lake St. Lucia. The authorities attempted to increase the fresh water
120 supply to the lake by excavating a canal (Mpempe Canal from near Mpempe Pan to 1 km south of Demazane Pan). Flooding
caused by Cyclone Domoina in 1984 resulted in severe erosion and the formation of a new stream between Tshanetshe Pan
and Mpempe Pan (Taylor, 1986). Additional dredging of a channel (Tshanetshe Canal) in 1986 by a local farmer (Neal, 2001)
resulted in the fact that today much of the Mkhuze River water is diverted through the Tshanetshe-Demazane Canal System
(Stormanns, 1987; Neal, 2001; Barnes et al., 2002; Ellery et al., 2003). Scientific evaluation of the actions taken and their
125 consequences for the system has been overwhelmingly negative (e.g., Alexander, 1973; Taylor, 1982b). However, Ellery et al.
(2003) not only provide a detailed description of the channelization processes in the Mkhuze Wetland System to which the
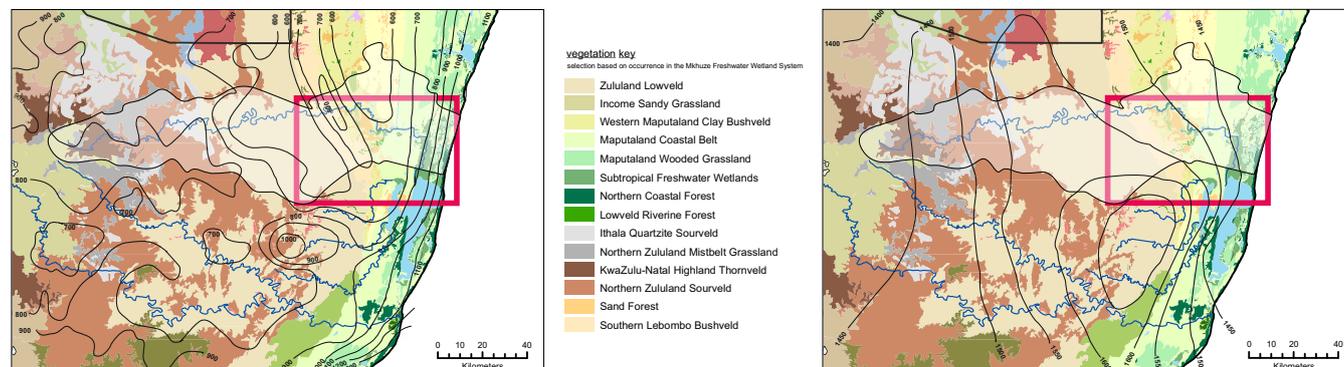
Figure 2. The vegetation coverage in the surroundings of the Mkhuze Wetland System is shown. The figure displays the entire catchment area of the Mkhuze River (represented by the outlined, lightened area). The red rectangle indicates the extent of the study area (see Figure 1). In addition to vegetation cover, precipitation isolines (left figure) and evaporation isolines (right figure, in mm/year) are overlaid (adopted from Taylor, 1982a).

reader is referred, but also emphasizes that the alteration of the Mkhuze River flow would also likely have occurred naturally. One aspect which is referred to the channelization processes is a change in vegetation cover. It is reported that formerly extensive stands of *Cyperus papyrus* within the floodplain area were reduced in extension and partly replaced by species which are tolerant to frequent inundation instead of permanently flooded conditions, such as *Cyperus natalensis* and *Echinochloa pyramidalis* (Stormanns, 1987; Neal, 2001).

2.2 Sampling

Collection of samples took place during a field campaign in November/December 2018. Ten plant samples were collected. If possible, replicate plant species were sampled at various sampling sites within the system. The different species were selected based on the occurrence of large cohorts in the field or based on high reported occurrences in previous studies (Stormanns, 1987; Neal, 2001), but not all major plant communities mentioned could successfully be sampled during the field campaign. These include aquatic plants from the *Nymphaceae* family (n = 2) as well as the aquatic plant *Phragmites australis* (n = 2) growing on both dry and flooded soils, two species of wetland grasses, namely *Vossia cupidata* (n = 2) and *Cynodon dactylon* (n = 2), and two representatives of the *Cyperaceaea* family, namely *Cyperus papyrus* (n = 1) and *Cyperus alternifolius* (n = 1). A total of 41 surface sediment samples (uppermost 10 cm) were collected along the course of the Mkhuze River and a transect extending into North Lake (northern part of Lake St. Lucia, Figure 1). The collection of sediment samples was conducted under permit from Ezemvelo KZN Wildlife and iSimangaliso Wetland Park Authority.

2.3 Laboratory Analyses

Figure 4 presents the different sample preparation steps in detail. All glassware used was combusted at 450°C for 5h prior to use.
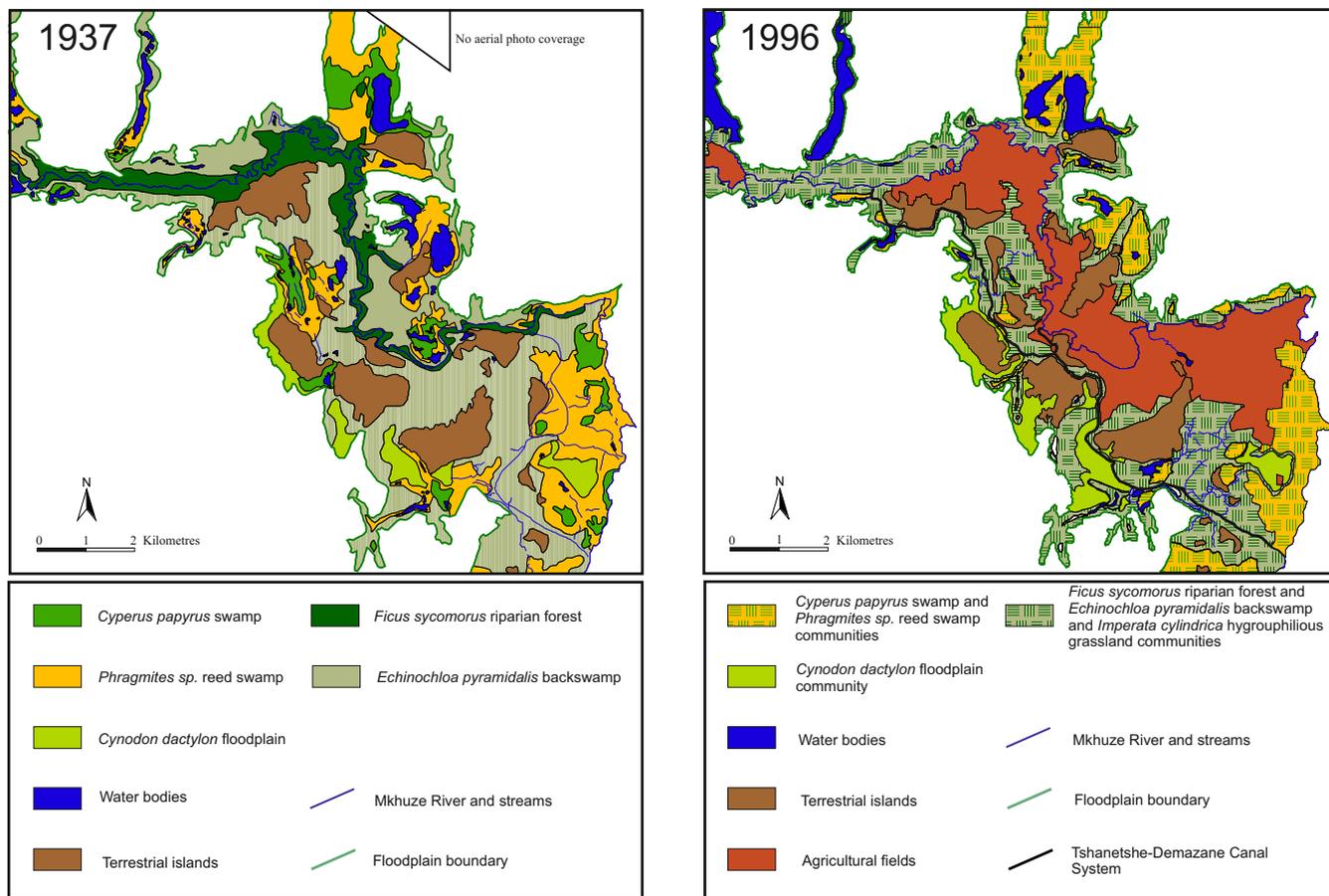
Figure 3. Distribution in the vegetation communities and land-use on the Mkhuze Floodplain in 1937 (left) and 1996 (right) (adopted from Neal, 2001).

2.3.1 Bulk organic matter analyses

Bulk organic analyses for determining total carbon and nitrogen content and bulk carbon isotope signatures were performed at MARUM, University of Bremen. About 10 mg of decalcified samples were wrapped in a tin capsule and analyzed with a continuous-flow elemental analyzer-isotope ratio mass spectrometer (ThermoFinnigan Flash EA 2000 coupled to a Delta V
150 Plus IRMS). The combustion oven (filled with quartz wool, chromium oxide, and silvered cobaltous-cobaltic oxide), in which C- and N-containing compounds are oxidized, was operated at 999 °C. This was followed by reduction of the resulting nitrogen gases in the reduction reactor (filled with quartz wool and copper reduced granulate) operated at 680 °C. Water formed was removed in a water trap (filled with magnesium perchlorate). Finally, N_2 and CO_2 were separated chromatographically (using an IRMS steel separation column for NC; length 300 cm, OD 6 mm, ID 5 mm, kept at 40 °C) and transferred on-line to IRMS
155 via a Conflow IV interface. Helium as carrier gas and oxygen as oxidation reagent were used at flow rates of 100 ml/min and
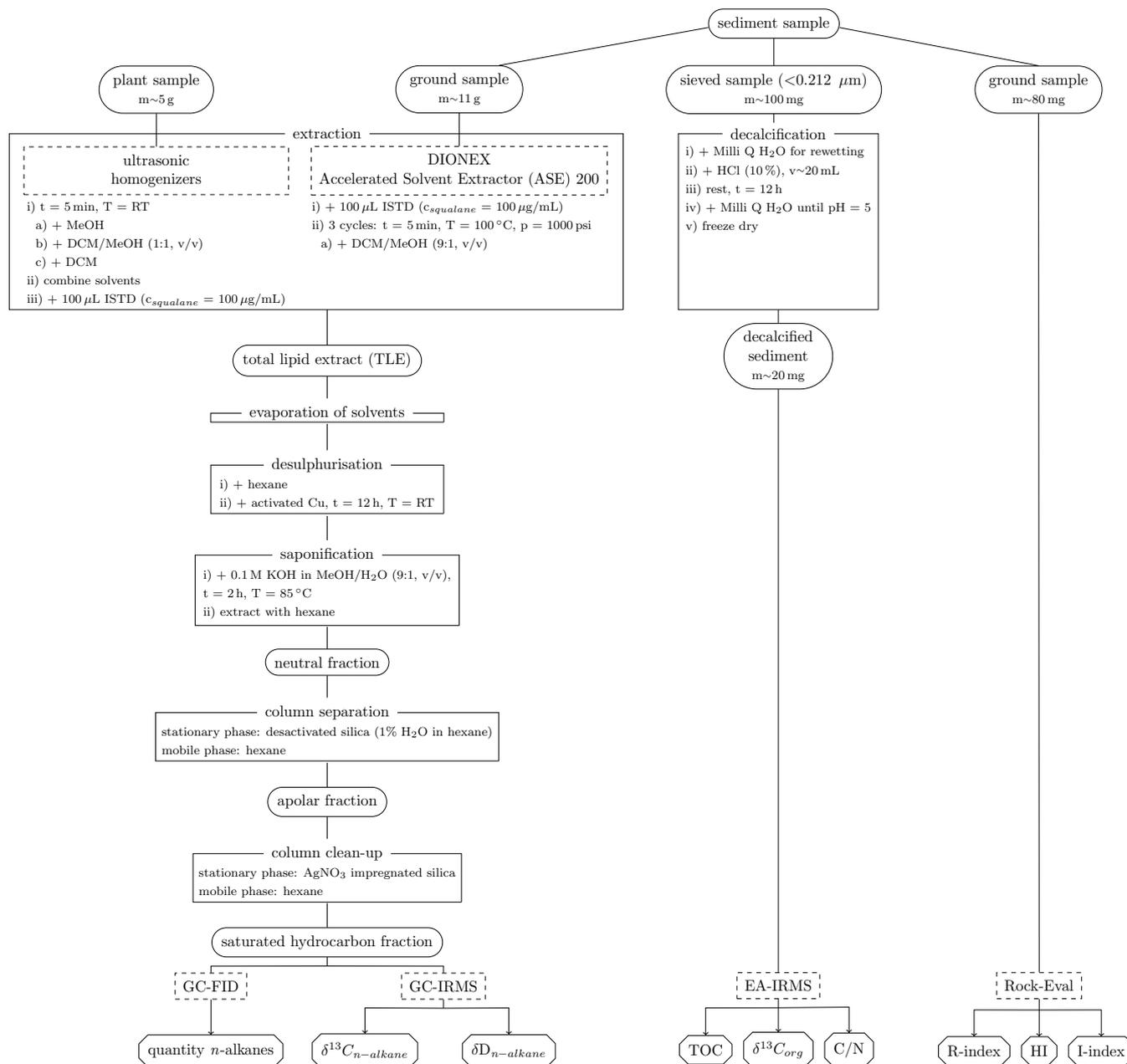
Figure 4. Overview of laboratory analyses. Rounded shapes display obtained sample fractions, rectangular shapes with solid lines display detailed sample preparation steps, rectangular shapes with dashed lines refer to specific devices, and octagonal shapes display acquired parameters.

Abbreviations used (in alphabetical order): **AgNO$_3$** silver nitrate, **c** concentration, **C/N** carbon to nitrogen ratio, **Cu** copper, **DCM** dichloromethane, **EA** elemental analyzer, **FID** flame ionization detector, **GC** gas chromatography, **H$_2$O** water, **HCl** hydrochloric acid, **HI** Hydrogen Index, **IRMS** isotope ratio mass spectrometer, **ISTD** internal standard, **KOH** potassium hydroxide, **m** mass, **MeOH** methanol, **p** pressure, **RT** room temperature, **t** time, **T** temperature, **TOC** total organic carbon.

200 ml/min, respectively. Primary standardization of the Delta V Plus IRMS was based on duplicate injections of a reference gas standard from a laboratory tank. The CO_2 reference gas ($\delta^{13}C = 34.17 \text{‰} \pm 0.1 \text{‰}$ vs Vienna Pee Dee Belemnite (VPDB), $5.0 \text{ V} \pm 0.5 \text{ V}$ at m/z 44) was calibrated using IAEA-CH-6 international standards. Quantification of total nitrogen and organic carbon was achieved by external standard calibration using peak areas that yielded a linear 5-point calibration curve. Re-

160 peated analysis of an internal laboratory standard cross-referenced to the certified IAEA-CH-6 international standard yielded a precision and accuracy of 0.2 ‰ each. Sample concentration data are reported blank corrected.

Thermal analyses were performed at IFP Energies Nouvelles Lab (Rueil-Malmaison, France) using a Rock-Eval® 6 device (Vinci Technologie). About 80 mg of the dry ground sample was pyrolyzed in an inert atmosphere (N_2) by heating from 200 °C to 650 °C at 25 °C/min, then residual carbon was combusted in air from 300 °C to 850 °C at 20 °C/min (Espitalie et al.,

165 1985; Disnar et al., 2003). Gases released were monitored by a flame ionisation detector (FID) for hydrocarbon compounds (HC), and by infrared detectors (IR) for CO and CO_2. Total Organic Carbon (TOC in wt-%), Mineral Carbon (MinC in wt-%), Hydrogen Index (HI in mg HC/g TOC^{-1}) and Oxygen Index (OI in mg CO_2/g TOC^{-1}) were calculated by integrating the amounts of HC, CO, and CO_2 produced during thermal cracking and combustion of OM ort thermal decomposition of carbonates between defined temperature limits (Behar et al., 2001; Lafargue et al., 1998). Since cracking temperature of organic

170 compounds depends on their structural stability, the thermal status of OM was characterized by combining R-index (i.e., relative contribution of most thermally stable HC pools) and I-index (i.e., ratio between thermally labile and resistant HC pools; details in Sebag et al., 2016). As derived from a mathematical construct, if the gradual decomposition of labile compounds is its main driver, OM composition can be described as a continuum from biological tissues to a mixture of organic constituents derived from OM decomposition and plotted along a linear regression line (called "Decomposition line"; Malou et al., 2020) in the

175 I-index vs R-index diagram (called thereafter I/R diagram; Albrecht et al., 2015). However, situations with OM mixture from different sources or where decomposition is so intense that it even affects the more thermally stable pools may generate a distribution diverging from the "Decomposition line". In addition, since decomposition temperature of carbonates depends on their composition, examination of CO_2 and CO thermograms enables to identify the carbonate minerals present in the mineral matrix (Pillot et al., 2014; Sebag et al., 2018).

180 ### 2.3.2 Determination of *n*-alkane concentrations

Analyses were performed using a FOCUS gas chromatograph coupled to a flame ionization detector (GC-FID). The GC oven hosted a Restek Rxi-5ms capillary column (30 m x 250 μm x 0.25 μm). The inlet temperature was set to 260 °C and splitless injection mode was used. The GC oven was set at 60 °C, held for two minutes, increased to 150 °C with a heating rate of 20 °C/min, subsequently followed by an increase of 4 °C/min to the final temperature of 320 °C, which was held for 11 minutes.

185 Quantification of the long-chain *n*-alkanes was performed by external standard calibration using the peak areas. The external standard used for this purpose contains *n*-alkanes (C_{19} to C_{34}) at a concentration of 10 ng/μL each and was measured repeatedly after all six samples, achieving a relative standard deviation of %RSD < 09.2 %. A blank sample containing only the internal standard (ISTD) and a double blank sample not containing the ISTD were also measured to ensure that no contamination occurred during the sample preparation and measurement.

2.3.3 Stable isotope analyses of *n*-alkanes

Compound-specific δ^{13}C values of the long-chain *n*-alkanes were determined using a TRACE GC Ultra equipped with an Agilent DB5/HP-5ms capillary column (30 m x 250 µm x 0.25 µm) coupled to a Finnigan MAT 252 IRMS via a combustion interface (operation at 1000 °C). The GC oven temperature was set at 120 °C, held for three minutes, and raised to the final temperature of 320 °C at a heating rate of 5 °C/min, held for 15 minutes. CO_2 was used as the reference gas. All samples were measured in duplicate if sufficient material was available, and values are given in ‰ VPDB. Standard deviations of replicate analyses of all odd-numbered *n*-alkanes analyzed (C_{23} to C_{35}) were less than 0.25‰ (C_{23}: 0.10‰ ± 0.07‰, C_{25}: 0.07‰ ± 0.05‰, C_{27}: 0.08‰ ± 0.06‰, C_{29}: 0.06‰ ± 0.06‰, C_{31}: 0.09‰ ± 0.06‰, C_{33}: 0.07‰ ± 0.06‰, C_{35}: 0.08‰ ± 0.06‰). Accuracy and precision were determined by analyses of an external *n*-alkane standard calibrated against the A4-Mix isotope standard (A. Schimmelmann, University of India) and measured repetitively every six samples. The precision (% RSD) and accuracy (bias compared to the offline value determined via elemental analysis) of the internal standard ($\delta^{13}C_{squalane}$ = -19.9‰ ± 0.3‰) were 1.6 % and -0.27‰, respectively. Compound-specific stable hydrogen isotope δD values were determined using a TRACE GC Ultra (column and temperature program are the same as for δ^{13}C) coupled to a Finnigan MAT 253 IRMS via a pyrolysis reactor (operating at 1420 °C). H_2 was used as the reference gas and all samples were measured as duplicates when sufficient sample volume was available. Reported values are in ‰ Vienna Standard Mean Ocean Water (VSMOW). Standard deviations of replicate analyses of all *n*-alkanes analyzed (C_{23} to C_{35}) were less than 3‰ (C_{25}: 1.0‰ ± 0.59‰, C_{27}: 1.08‰ ± 0.67‰, C_{29}: 0.49‰ ± 0.54‰, C_{31}: 0.46‰ ± 0.46‰, C_{33}: 0.62‰ ± 0.46‰, C_{35}: 0.68‰ ± 0.56‰). Accuracy and precision were determined by analyses of an external *n*-alkane standard calibrated against the A4-Mix isotope standard (A. Schimmelmann, University of India) measured repeatedly every six samples. The precision (%RSD) and accuracy (bias compared to the offline value) of the internal standard (δD$_{squalane}$ = -180‰ ± 3‰) were 1.4 % and 0.03‰, respectively. The H3 factor was repeatedly measured and gave a value of 4.8 ± 0.1 over the whole measurement series.

2.4 Distributional parameters of *n*-alkanes

The carbon preference index (CPI) and the average chain length (ACL) were adapted from Cooper and Bray (1963) and Poynter and Eglinton (1990), respectively. The following calculations were made:

carbon preference index: $CPI = 0.5 * \left[\frac{\sum_{23}^{33} C_{odd}}{\sum_{22}^{32} C_{even}} + \frac{\sum_{25}^{35} C_{odd}}{\sum_{24}^{34} C_{even}} \right]$

average chain length: $ACL = \frac{\sum_{23}^{35} i * C_{i,odd}}{\sum_{23}^{35} C_{i,odd}}$

relative concentration (contribution) [%]: $C_x = \frac{C_x}{\sum_{23}^{35} C_{even,odd}}$

Table 1. Chemical parameters of sedimentary bulk organic matter: total organic carbon content (TOC) in % dry weight (DW), carbon to nitrogen ratio (C/N), summed concentration of medium to very-long chain plant wax-derived *n*-alkanes normalized to dry weight and organic carbon (OC), and bulk organic carbon isotopic composition in per mil in reference to Vienna Pee Dee Belemnite.

	TOC	C/N	$\sum conc_{C_{22}-C_{35}}$	$\sum conc_{C_{22}-C_{35}}$	$\delta^{13}C_{org}$
sub-environment	[% DW]	(mass)	[μg/g DW]	[μg/g OC]	[‰]
upper reach	1.8 ± 0.5	11.8 ± 1.0	7.0 ± 0.8	280.2 ± 165.0	-21.87 $\pm$ 3.84
floodplain	3.2 ± 2.6	14.7 ± 2.7	2.9 ± 3.4	124.5 ± 81.7	-19.65 $\pm$ 1.19
swamp	4.6 ± 2.7	14.1 ± 2.1	4.7 ± 2.9	114.3 ± 32.9	-20.86 $\pm$ 0.86
delta	1.5 ± 0.3	11.4 ± 1.4	1.6 ± 0.8	89.0 ± 23.3	-19.66 $\pm$ 0.45
lake	1.6 ± 0.1	12.9 ± 1.2	1.8 ± 0.3	119.5 ± 20.2	-19.36 $\pm$ 0.73

Displayed are the median and the median absolute deviation of analyzed parameters.

2.5 Statistical Analyses

All statistical analyses were performed using R software (R version 4.0.3 and RStudio version 1.4.1103). To test whether statistically significant differences occurred between the sub-environments, the Kruskal-Wallis test was performed using the stat_cor_mean() function of the "ggpubr" package (version 0.4.0). When the *p* value indicated that differences (*p*<0.05) between sub- nvironments were evident, the test was supplemented with a pairwise Wilcoxon rank sum test (base package "stats") to determine which sub-environments had significant differences between them. The Benjamini and Hochberg "BH" method was used to adjust p-values. Correlation coefficients were calculated by using the stat_cor function with the default Pearson method of the "ggpubr" package (version 0.4.0). Box-and-whisker plots were generated using the "ggplot2" system (version 2.3.3.3) of the "tidyverse" package (version 1.3.0) and "ggpubr" (version 0.4.0) and the geom_boxplot() function implemented here. Here, the median of the respective data is shown as a solid line, the box of the boxplot ranges from the lower to the upper hinges corresponding to the first (25th percentile) and third (75th percentile) quartiles. Here, the median of the respective data is shown as a solid line and the lower and upper hinges correspond to the first (25th percentile) and third (75th percentile) quartiles. The lower/upper whisker extends from the lower/upper hinge to the smallest/largest value if it is not smaller/larger than 1.5 times the interquartile range from the hinge. Otherwise, the respective data point is drawn as a single point representing an outlier. For the principal component analysis (PCA) performed, missing values of the data set were first imputed using the impute.PCA() function and applying the regularized iterative PCA algorithm of the "missMDA" package (version 1.18). Subsequently, the actual PCA calculations were performed by using the prcomp() function (base package "stats").

3 Results

3.1 Chemical parameters of bulk organic matter

Total organic carbon (TOC), as a measure of organic matter (OM) content, increased in surface sediments from the upper reach

240   to the swamp sub-environment, where samples contained the highest amounts of TOC ranging from 0.9 % to 8.1 % (Table 1). Higher variance is observed for the upper reach, floodplain, and swamp sub-environment, compared to very narrow ranges of values in the delta (1.4 % - 1.8 %) and lake sub-environment (1.4 % - 1.7 %). Samples from the floodplain and swamp sub-environments show significantly higher C/N ratios compared to the other sub-environments (p < 0.05, Table 1).

To estimate the total amount of plant wax input to the sub-environments, the sum of the concentrations of all long-chain odd-

245   numbered n-alkanes was considered (Table 1). When normalized to sample mass, delta and lake samples contained significantly lower amounts of plant wax-derived lipids compared to swamp samples (p < 0.005). However, when normalized to organic carbon, no significant differences were detected between any of the sub-environments investigated (p > 0.05).

Bulk OM δ^{13}C shows more depleted values in the samples from the upper reach and the swamp sub-environments than in the other sub-environments, but statistical evidence is present only for the distinction between the swamp sub-environment and

250   the delta/lake sub-environment (p < 0.05).

3.2 Thermal analysis of bulk organic matter

The HI values show a decreasing trend from the upstream (ca. 115 mg HC/g TOC^{-1} for upper reach and 100 mg HC/g TOC^{-1} for floodplain; Figure 6 A) to the downstream sub-environments (ca. 75 mg HC/g TOC^{-1} for swamp and delta; ca. 60 mg HC/g TOC^{-1} for lake; Figure 6 A). The range around the mean value is generally small (ca. 25 mg HC/g TOC^{-1}), except for floodplain sam-

255   ples which displayed a high variability, ranging between ca. 50 and 135 mg HC/g TOC^{-1}, (Figure 6 A).

The R-index values show a comparable pattern with decreasing mean values from upstream (> 0.60 for upper reach and floodplain; Figure 6 B) to downstream sub-environments (< 0.60 for swamp, delta and lake; Figure 6 B). The highest values were measured in floodplain samples (> 0.65, Figure 6 B, while swamp samples displayed the highest variance splitting into two groups (ca. 0.55 and 0.65, Figure 6 B).

260   The I-index values revealed an inverse pattern with low values in upstream sub-environments (ca. 0.1 for upper reach and floodplain, Figure 6 C), high values for the downstream sub-environments (ca. 0.3 for delta and lake, Figure 6 C) and swamp samples divided into two groups (ca. 0.06 and 0.22, Figure 6 C).

In the I/R diagram (Figure 7) the studied samples projected onto the "decomposition line" describing the linear relationship between R and I when the gradual decomposition of the most labile constituents controls the OM transformation (i.e., stabi-

265   lization). Lake and delta samples contain the most labile OM (R < 0.57 and I > 0.25, Figure 7) while upper reach and floodplain samples contain the most stable OM (R > 0.62 and I < 0.25, Figure 7) with swamp samples falling in between these extremes (Figure 7). It is important to highlight that floodplain and swamp samples display high dispersion around the "decomposition line" in comparison with the strong correlation (R^2 > 0.9) usually observed for composts, litters, and topsoils (Albrecht et al., 2015; Sebag et al., 2016).
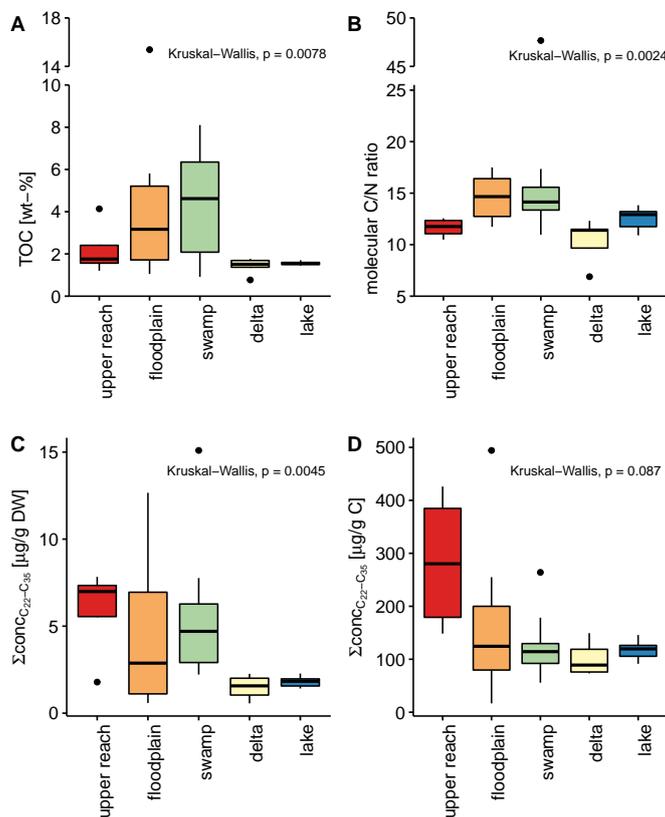
Figure 5. Box-and-whisker plots show total organic carbon content as a percent of dry weight (**A**), carbon to nitrogen ratios (**B**), summed concentration of long-chain *n*-alkanes normalized to dry weight (**C**), and summed concentration of long-chain *n*-alkanes normalized to organic carbon (**D**) of all surface sediments. The colours of each box refer to the assigned sub-environments of the Mkhuze Wetland System. *Note that the y-axis of **A** and **B** is broken.*

3.3 Distribution patterns and stable carbon isotopic composition of *n*-alkanes

All surface sediment samples analyzed contained long-chain, odd-numbered *n*-alkanes (C_{23} to C_{35}). The carbon preference index (CPI) has average values of 6.7 ± 1.5 for all surface sediments, confirming that *n*-alkanes originated from plant waxes due to the characteristic odd-over-even dominance. The CPI of the collected plant samples was 9.8 ± 5.5. The average chain length (ACL) for surface sediment samples was 30.2 ± 0.6, reflecting the high proportion of longer-chain *n*-alkanes, and 29.1 ± 1.7 for plant samples. Both parameters showed no statistically significant difference when comparing the sub-environments.

3.3.1 Plant samples

The sampled plants can be distinguished from each other based on their relative *n*-alkane distribution patterns and corresponding δ^{13}C signatures. Aquatic plants belonging to the *Nymphaceaea* family (common water lilies) show a symmetrical
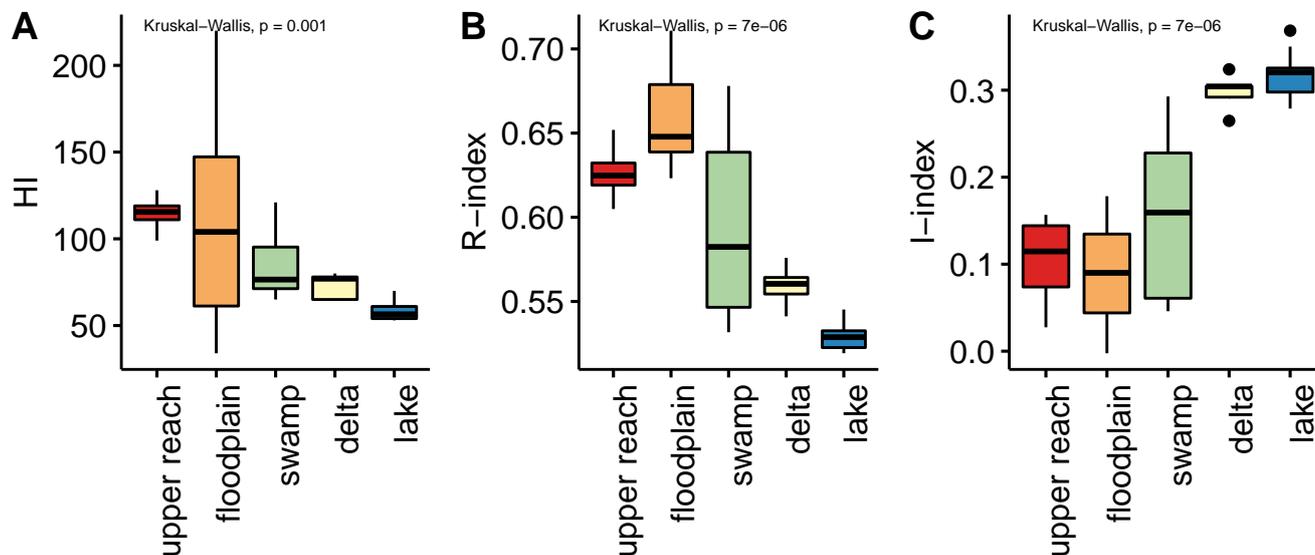
Figure 6. Displayed are the indices determined by Rock Eval analyses. Hydrogen Index (HI, **A**), R-index (**B**), and I-index (**C**), as introduced by Sebag et al. (2016) are displayed grouped by assigned sub-environments (see Figure 1 and section 2.1.1) of the Mkhuze Wetland System.

distribution around the two dominant n-alkanes C_{27} (31.2 % $\pm$ 0.7 %) and C_{29} (33.0 % $\pm$ 4.8 %) (Figure 8 A). Similarly, *P. aus-*
280 *tralis* (common reed), an emergent aquatic plant species, also shows high concentration of the C_{27} n-alkane (22.1 % $\pm$ 1.2 %), but the dominance of C_{29} (41.9 % $\pm$ 9.9 %) determines the n-alkane distribution pattern (Figure 8 B). Based on their stable carbon isotope signatures, these aquatic plants are classified as C_3 plants (*Nymphaceaea*: $\delta^{13}C_{C_{31}}$ = -30.60 ‰ $\pm$ 0.61 ‰, *P. australis*: $\delta^{13}C_{C_{31}}$ = -34.99 ‰ $\pm$ 0.55 ‰).

The C_4 ($\delta^{13}C_{C_{31}}$ = -20.53 ‰) wetland sedge *C. papyrus* (common papyrus, Figure 8 C) shows a symmetrical distribution
285 around the dominant n-alkane C_{31} (31.9 %) accompanied by comparatively similar contributions of the n-alkanes C_{29} (19.5 %) and C_{33} (12.8 %). It is striking that the sum of the relative concentrations of the long-chain, odd-numbered n-alkanes is just over 70 %, the remaining is accounted for by the respective even-numbered n-alkanes, of which C_{32} (15.3 %) has the largest share. The distribution pattern of another *Cyperaceae* species, namely the C_3 ($\delta^{13}C_{C_{31}}$ = -38.87 ‰) plant *C. alternifolius* (umbrella papyrus, Figure 8 D), is characterized by predominantly the C_{31} n-alkane (66.1 %).

290 Wetland grasses, such as C_4 ($\delta^{13}C_{C_{31}}$ = -18.66 ‰ $\pm$ 0.21 ‰) plant *V. cuspidata* (hippo grass, Figure 8 E) exhibits co-dominant concentrations of the n-alkanes C_{27} (27.9 % $\pm$ 0.9 %) and C_{29} (26.8 % $\pm$ 2.3 %) homologues going along with the occurrence of the very-long-chain n-alkanes C_{31} (11.7 % $\pm$ 1.6 %), C_{33} (8.9 % $\pm$ 2.5 %), and C_{35} (9.4 % $\pm$ 1.5 %). *C. dactylon* (bermuda grass, Figure 8 F) another C_4 ($\delta^{13}C_{C_{31}}$ = -22.10 ‰ $\pm$ 0.06 ‰) wetland grass is clearly determined by the low dis-persion around the dominant very-long-chain n-alkane C_{33} dictating the appearance of the distribution with a 56.7 % $\pm$ 8.8 %
295 share (C_{31} = 23.5 % $\pm$ 11.8 % and C_{35} = 8.1 % $\pm$ 6.5 %).
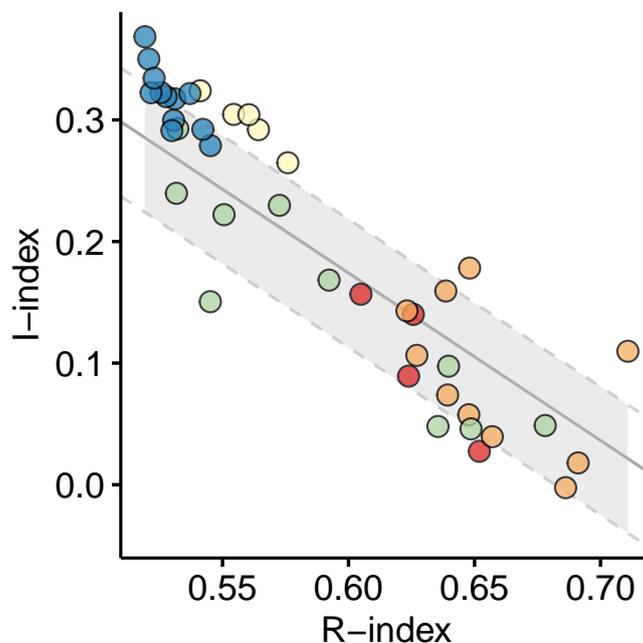
14

Figure 7. I/R diagram. The colour of the circles reflects the sub-environment (see Figure 1 and section 2.1.1) origin of the sedimentary organic matter: red = upper reach, orange = floodplain, green = swamp, yellow = delta, and blue = lake. The grey shaded area refers to the linear regression describing the continuum from biological tissue to a mixture of decomposition constituents ("decomposition line", Malou et al., 2020).

3.3.2 Surface Sediments

Figure 9 shows the relative concentrations of *n*-alkanes and their stable isotopic signatures for carbon and hydrogen in surface sediments within each sub-environment of the Mkhuze wetland. For simplicity, not all individual *n*-alkanes are displayed, but a reduced representation is shown. For reduction, the individual *n*-alkanes are grouped so that only the parameters of their representatives are shown to illustrate the exemplary trends. This grouping was made on the basis of visual criteria (trends across the wetland system) and verified by statistical means. The results of a principal component analysis (not shown) provide information about variables that contain redundant information. For further validation, the coefficients of the linear correlation between the individual variables were used. All methods show that the following grouping is justified: (i) the parameters shown for the C_{25} *n*-alkane also reflect trends in the C_{23} *n*-alkane (contribution: $R^2 = 0.72$, $p < 0.001$, $\delta^{13}C$: $R^2 = 0.91$, $p < 0.001$); (ii) the shown parameters of the C_{29} *n*-alkane also reflect the trends of the C_{31} *n*-alkane (contribution: $R^2 = 0.61$, $p < 0.001$; $\delta^{13}C$: $R^2 = 0.86$, $p < 0.001$; δD: $R^2 = 0.66$, $p < 0.001$); and (iii) the presented parameter trends of the C_{33} *n*-alkane are also representative for the C_{35} *n*-alkane (contribution: $R^2 = 0.55$, $p < 0.001$, $\delta^{13}C$: $R^2 = 0.95$, p textless 0.001). The C_{27} homologue show a correlation with both C_{25} ($\delta^{13}C$: $R^2 = 0.90$, $p < 0.001$; δD: $R^2 = 0.78$, $p < 0.001$)) and C_{29} ($\delta^{13}C$: $R^2 = 0.90$, $p < 0.001$;
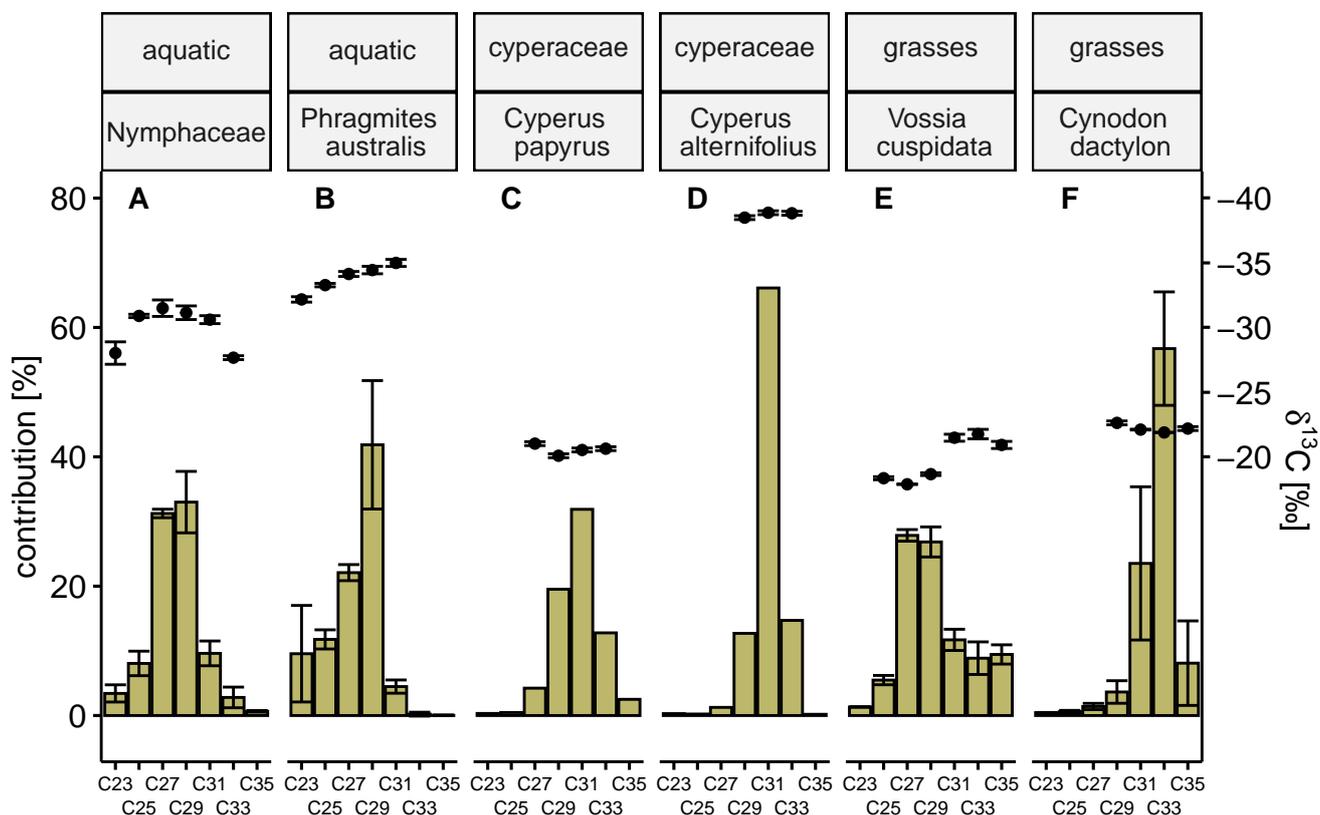
15

Figure 8. Green coloured bars show the relative concentration of long-chain, odd-numbered n-alkanes ($C_{23} - C_{25}$) of *Nymphaceaea* **A**, *Phragmites australis* **B**, *Cyperus papyrus* **C**, *Cyperus alternifolius* **D**, *Vossia cupidata* **E**, and *Cynodon dactylon* **F**. Black circles represent corresponding carbon isotope values in reference to Vienna Pee Dee Belemnite (‰ VDPB) of each n-alkane. Error bars represent the respective standard deviation. When no standard deviation could be determined, intra-laboratory long-term errors were used instead (± 0.3 ‰).

δD: $R^2 = 0.82$, $p < 0.001$) for the stable isotope values, but no stronger correlation in terms of relative contribution to any of the

310   homologues ($R^2 < 0.5$).

The medium-chain n-alkanes C_{23} and C_{25} show an increasing contribution downstream (upper reach → floodplain → swamp → delta → lake), the contribution of C_{25} ranging from $1.5\% \pm 0.3\%$ in the upper reach sub-environment to $5.4\% \pm 0.9\%$ in the lake sub-environment (Figure 9 A). The corresponding stable carbon isotope signatures show a C_3/C_4 mixed signal (Figure 9 D) with enhanced influence of C_3 vegetation in the upper reach, and swamp sub-environments, respectively (Figure 9 D).

315   δD values show similar ranges for the upper reach to the swamp sub- environment with a slight decrease in mean values downstream and more enriched values in samples from the delta and lake sub-environment (Figure 9 G).

The long-chain n-alkanes C_{29} and C_{31} show similar contributions to all sub-environments (C_{29}: $13.6\% \pm 2.1\%$, C_{31}: $22.1\% \pm 2.1\%$), except for a significantly stronger contribution in the upper reach samples (C_{29}: $18.4\% \pm 2.1\%$, C_{31}: $28.8\% \pm 3.1\%$; $p < 0.05$,

Figure 9 B). The corresponding stable carbon isotope signatures show a stronger influence of C_3 vegetation (Figure 9 E).

320 Decreasing mean δD values were observed from the upper reach sub-environment (mean $\delta D = 140.8\,‰$, Figure 9 H) to the swamp sub-environment (mean $\delta D = 153.3\,‰$, Figure 9 H). The hydrogen isotopic composition of the long-chain n-alkanes in the downstream lake sub-environment (Figure 9 H) were in contrast significantly higher (mean $\delta D = 133.9\,‰$) compared to the swamp and floodplain sub-environments ($p < 0.05$).

The very-long-chain n-alkanes C_{33} and C_{35} contribute on average $22.6\,\% \pm 3.8\,\%$ (C_{33}) and $6.5\,\% \pm 1.7\,\%$ (C_{35}) to all

325 sub-environments, with a maximum contribution in samples from the swamp region (C_{33}: $27.6\,\% \pm 7.5\,\%$, C_{35}: $8.8\,\% \pm 1.2\,\%$, Figure 9 C). Carbon isotopic values of the very-long-chain n-alkanes show a large C_3 vegetation influence in the upper reach sub-environment, large variance in the floodplain sub-environment associated with a strong C_4 influence that decreases slightly thereafter (Figure 9 F). The hydrogen isotopic composition was similar across all sub-environments, apart from the lake samples which were characterized by elevated values (Figure 9 I).

330   4   Discussion

4.1   Plants *n*-alkane distribution patterns as indicators of variable hydrological conditions

Differences in *n*-alkane distribution patterns between plant species have previously been observed in numerous studies (Ficken et al., 2000; Carr et al., 2014; Badewien et al., 2015; Liu et al., 2018). We are aware that the use of *n*-alkane distribution patterns to distinguish plant species and chemotaxonomic fingerprinting approaches are more controversial when transferring findings

335 from one area to another, as it has been shown that variations can also occur within specific species and even between plant parts of the same species (Bush and McInerney, 2013). Because all investigated plants, however, are from the same system and, when possible, multiple plants of the same species were sampled in different sub-environments of the wetland system, we believe that influences such as variability due to different climatic growing conditions and intra-species variability is small.

Aquatic plant species such as the floating *Nymphaceae spp.* (common water lily) and the emergent wetland sedge *P. australis*

340 (common reed) (both C_3; Figure 8 A and B) show elevated concentrations of the medium-chain *n*-alkanes (C_{23} and C_{25}), making them distinguishable from other terrestrial higher plants, which is consistent with previous studies (Baas et al., 2000; Ficken et al., 2000; Liu et al., 2019). These aquatic plant species are found primarily in stagnant or slow flowing waters.

The riparian zone along the Mkhuze River is dominated by typical woody plants of riparian forests, such as *A. xanthophloea* (fever tree) and *F. sycomorus* (Sycamore fig) (Neal, 2001). While no representative of these species was sampled in this study,

345 woody plants, such as trees, are generally well studied (Vogts et al., 2009). Tropical C_3 trees are typically characterized by high C_{29} and C_{31} *n*-alkane contributions (in sum $> 75\,\%$), while the adjacent homologues show concentration mainly below $5\,\%$. However, the distribution patterns of *n*-alkanes show that this criterion can also be fulfilled by plants that cannot be described as woody, so that the interpretation of these specific alkanes should always be confirmed through further information, e.g., dominant vegetation form, hydrological conditions.
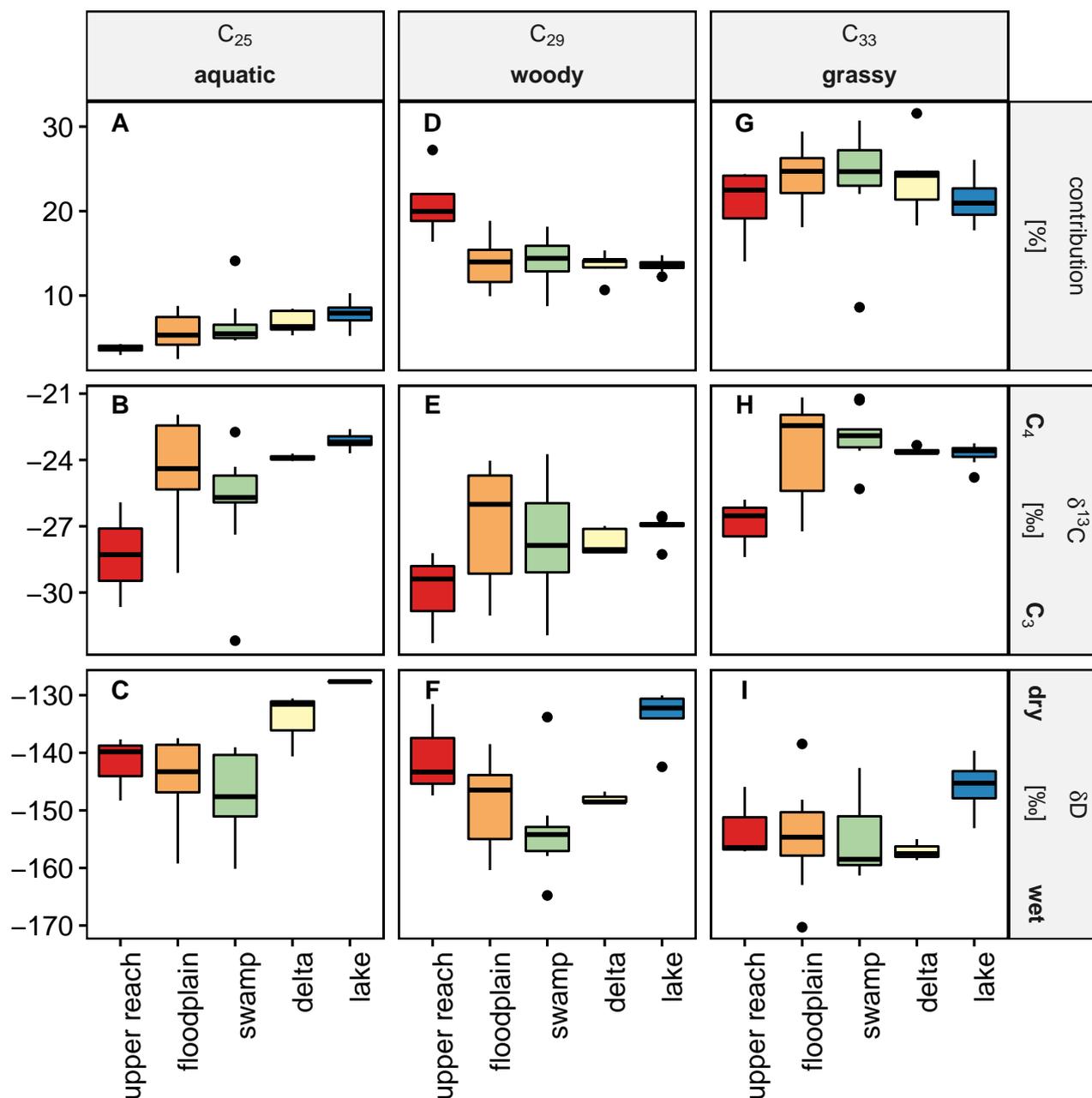
Figure 9. Box-and-whisker plots show the relative concentration in % **A**, **D**, **G**, carbon isotope signatures with respect to VPDB in ‰ **B**, **E**, **H**, and hydrogen isotope signatures with respect to VSMOW in ‰ **C**, **F**, **I** of the *n*-alkanes C_{25}, C_{29}, and C_{33} as representatives for the groups of *n*-alkanes classified as aquatic, woody, and grassy.

350   The wetland sedges *C. papyrus* (Papyrus; C_4) and *C. alternifolius* (Umbrella papyrus; C_3) (Figure 8 C and D) predominantly produce C_{31} *n*-alkanes, a finding consistent with the limited data available (Collister et al., 1994). Their natural occurrence is restricted to permanently flooded soils.

   C_4 grasses such as *V. cuspidata* (hippopotamus grass) or *C. dactylon* (Bermuda grass) (Figure 8 E and F), like many (sub)tropical grasses, are characterized by the production of the very long-chain *n*-alkanes (C_{33} and C_{35}) (Rommerskirchen

355   et al., 2006; Vogts et al., 2012). These wetland grasses are mostly tolerant of intermittent soil flooding and other disturbances (Holm et al., 1977), so they generally occur widely.

4.2   Spatial comparison of organic matter characteristics in surface sediments

Clear differences between the individual sub-environments of the Mkhuze Wetland System become evident by comparing the organic matter characteristics with respect to stability, degree of degradation, primary contributing vegetation and its hydro-

360   logical growth conditions. That these differences sometimes appear small in absolute values is attributable to the system itself. The discussed sub-environments (see section 2.1.1) cannot be separated from each other by sharp boundaries but rather the transition show gradual transitions in their ecological manifestations. That the characteristics of the OM differ from one another despite this gradual transformation underscores the importance of the individual environments to the system.

   The term stability of OM refers to the bioavailability of the OM to microbial decomposers and is controlled by different

365   factors (chemical or physical properties or environmental factors). The combination of thermal and chemical assessments of the biogeochemical stability allows to shed light on the different underlying processes. The expression of stability ranges from labile, i.e., easily microbially degradable to stable/refractory, i.e. hardly or not microbially degradable. Rock-Eval® analyses addresses the thermal stability by assessing the quality of OM through (i) the amount of hydrocarbons released per gram organic carbon (Hydrogen Index) and (ii) different thermally stable portions of the fraction released (through R- and I-indexes). The

370   chemical stability can be addressed with the carbon to nitrogen ratio (C/N) which in terrestrial systems is mostly interpreted in a process-oriented manner (Reuter et al., 2020; Reddy and DeLaune, 2008, and references therein). Fresh OM, such as plant debris often shows very high C/N ratios, approaching a value of 10 during decomposition, which is due to dilution with bacterial biomass, which decomposes the organic matter and uses it to build up further biomass and produce energy through mineralization, having a C/N ratio of 10.

375   The concentration of plant wax-derived *n*-alkanes, biomarkers that are characterized by their high refractory properties, also elucidates information on stability and quality of the organic matter. When comparing their concentration normalized to dry weight and organic carbon, respectively, conclusions about whether they either reflect remnants of degraded OM leading to their relative enrichment or input of fresh OM can be drawn.

   Plant wax *n*-alkane distributions and associated stable isotopic signatures (see subsection 4.1 as plant characteristics are used

380   as a system's vegetation in-situ calibration to assess the dominant source vegetation.

4.2.1 Upper reach of the Mkhuze River

Bulk organic matter in surface sediments of the upper reach is generally low in concentration (see Table 1 and Figure 5 A) and shows geochemical and thermal characteristics of degraded OM (HI $\cong$ 120 mg/g TOC, C/N = 11.8 $\pm$ 1.0; Figure 6 A and Figure 5 B), which can be related to an advanced decomposition of thermally labile constituents (R $\cong$ 0.63, I = 0.15, linear

385 distribution within the limits of the "decomposition line" in the I/R diagram, Figure 7). The concentration of n-alkanes from plant waxes per dry weight and organic carbon is highest in the surface sediments of the upper reach (Table 1 and Figure 5 C-D) suggesting relative enrichment due to OM degradation. The relative contribution of long-chain n-alkanes C_{29} and C_{31} (Figure 9 D) is also highest, suggesting that sedimentary OM of the upper reach is dominated by inputs of woody plant sources. This is corroborated by the lowest stable carbon isotope values (C_3 plant origin) of all sub-environments (Figure 9 B, E, H).

390 OM in the surface sediments of the upper reach therefore reflect allochthonous contributions from the hinterland, since the Mkhuze River is primarily lined with riparian forests (Neal, 2001). These trees do not tolerate flooding or water saturated soil conditions so that they are found on the elevated channel levees. This interpretation of the hinterland as origin is further supported by the stable hydrogen isotopes of the respective n-alkanes, particularly evident in C_{29} (Figure 9 F). The relatively enriched δD values suggest that the plants producing them were exposed to relatively dry conditions during their growth phase.

395 These dry conditions are met to a large extent in the hinterland, considering that the precipitation gradient across the Mkhuze Wetland System is nearly halved from 1000 mm/year in the east near the coast to 600 mm/year at the Lebombo Mountains (Maud, 1980, Figure 2).

4.2.2 Floodplain

Bulk organic matter in surface sediments of the floodplain is characterized by high variability in both quantity (TOC, Table

400 1 and Figure 5 A) and quality (HI, R- and I-indexes, Figure 6 A-C). It splits into three groups, the first one corresponds to samples poor in OM (TOC < 1.5 %) and in hydrocarbon compounds (HI < 80 mg HC/gTOC). A second group corresponds to samples rich in OM (TOC > 5 %) and hydrocarbon compounds (HI > 150 mg HC/gTOC). The third group presents an intermediate situation (TOC≈2-3 %, HI ≈ 100 mg HC/g TOC). An explanation could consider that this gradual evolution corresponds to a more or less advanced degradation of the sedimentary OM. However, the I-index does not support this interpretation, since

405 the samples with the lowest HI present the least advanced degree of decomposition of thermally labile compounds (I > 0.1), and conversely. In addition, floodplain samples show a wide dispersion in the I/R diagram (Figure 7) which excludes a gradual decomposition. By analogy with previous work on soils, such nonlinear signatures would rather be associated with OM mixtures of varying quality and origin, which is consistent with such a heterogeneous depositional environment.

Mixing of OM is further corroborated by the plant wax concentration per dry weight and organic carbon (Table 1 and Figure

410 5 C-D) showing great variances and therefore that n-alkanes are partly relatively enriched during degradation of OM but also inputs of fresh organic material which is in line with elevated C/N ratios (Figure 5 B).

High variability is also evident in the relative contributions of the n-alkanes (Figure 9 A, D, G) and the corresponding isotopic signatures (Figure 9 B, E, H) suggesting a mixture of OM of different origin. The floodplain of the Mkhuze Wetland

System is characterized by a mosaic of different smaller wetland types, ranging from the locally distinct river channel to

415 seasonally flooded areas to permanent (open) water bodies. The ecologically complex and variable diversity is reflected in all the parameters. However, it is noteworthy, despite this predominant scatter, that the strongest input of C_4 vegetation is clearly observed in floodplain sedimentary organic matter (Figure 9 B, E, H). This cannot be explained solely by the occurrence of C_4 grasses such as *C. dactylon* or *Echinochloa pyramidalis*, which are recognized as important floodplain vegetation communities (Neal, 2001), since the "grassy" *n*-alkane input is not significantly higher than in the downstream swamp (Figure 9 G). In

420 addition, Neal (2001) describes the floodplain is increasingly used for growing crops, such as the C_4 crops sugarcane or corn (Figure 3), which could explain the particularly strong C_4 signal.

4.2.3 Swamp

The bulk organic matter in surface sediments of the swamp sub-environment is similarly characterized by high variability in both quantity (TOC, Table 1 and Figure 5 A) and quality (HI, R- and I-indexes, Figure 6 A-C). As for floodplain sam-

425 ples, swamp samples are separated into three groups depending on their OM and hydrocarbon content with both contents decreasing downstream suggesting a more or less advanced degradation of the sedimentary OM. Similar to the floodplain sub-environment, the I-index oppose this assumption, as the samples with lowest HI (HI < 75) go along with the least advanced degree of decomposition (I > 0.2) pointing towards a mixture of OM related to overprinting of fluvially introduced OM by in-situ produced OM. The I/R diagram, while samples being globally aligned with the "decomposition line", also reveals two

430 distinct clusters showing a degraded and much less degraded signature, respectively. These results indicate that the swamp sub-environment contains a wide range of situations, as those similar to upstream (upper reach, floodplain) and downstream (delta, lake) sub-environments, and therefore reflects a transitional sub-environment.

Furthermore, the organic matter is characterized by comparatively high C/N ratios, i.e., corroborating addition of in-situ produced organic matter to the samples. This is also seen in the summed concentration of *n*-alkanes normalized to dry weight

435 being very high, while normalized to organic carbon being rather low what is attributed to fresh organic matter inputs.

A similar pattern like for the bulk organic matter can also be observed in the plant wax data. While the *n*-alkane distribution closely resembles that of the floodplain (Figure 9 A, D, G), the corresponding carbon isotope signatures (Figure 9 B, E, H) show a slightly lower influence of C_4 vegetation, but rather a mixed C_3/C_4 signal with slightly increasing C_3 vegetation influence downstream. This can be explained by the input of the locally dominant vegetation into the sedimentary organic

440 matter (overprinting), yet to a moderate extent. The Mkhuze Swamps are dominated by the C_3 wetland sedge *P. australis* (Figure 8 B) occurring along the eastern margin and large stands of the C_4 wetland grass *C. dactylon* (Figure 8 F) western side of the river channel. Although the hydrogen isotope signatures of the respective *n*-alkanes (Figure 9 C, F, I) indicate slightly wetter growth conditions compared to the floodplain, the differences are comparatively moderate.

4.2.4 Delta and lake

445 The organic matter of the lake and delta samples shows striking differences when compared with that of the upstream sub-environments of the Mkhuze Wetland System.

The bulk organic matter in surface sediments shows a homogeneous signature with lowest contents in OM (TOC < 1.6 %, Table 1 and Figure 5 A) and hydrocarbon compounds (HI < 80 mg HC/g TOC, Figure 6 A) of all sub-environments, and a high degree of preservation of thermally labile fractions (I > 0.3, partly in the upper limit of the "decomposition line"). These results

450   differ drastically from the OM results of the upstream sub-environments, but they do not reflect aquatic autochthonous contributions (as indicated by the low HI). Although the sources of this OM are probably terrestrial, it is not a detrital (allochthonous) OM, reworked from the catchment area, but rather a proximal (para-autochtonous) contribution.

The concentration of *n*-alkanes normalized to dry weight is comparatively low, but normalized to organic carbon no differences are observable, signifying the input of fresh material.

455   In contrast to bulk OM, the contribution of aquatic, woody, and grassy *n*-alkanes (Figure 9 A, D, G) and the corresponding C_3/C_4 signatures (Figure 9 B, E, H) are not significantly different from the upstream sub-environments. This implies that the sources of plant waxes regarding vegetation type are similar or possibly even the same as upstream. The narrow spread of stable and bulk carbon isotope signatures (Figure 9 B, E, H and Table 1) suggests that OM may be attributable to contributions from a restricted range of plant species. However, the associated hydrogen isotope signatures (Figure 9 C, F, I) indicate that the

460   contributing plants experienced completely different hydrological conditions during growth than plants in the upstream sub-environments. The *n*-alkanes in the lake surface sediments have a higher median δD compared to that of the upstream swamp by about 10 ‰ (C_{31}) to 20.0 ‰ (C_{29}). These significantly higher δD values indicate that the contributing vegetation used a different water source. Given the geomorphological and climatic characteristics of Lake St. Lucia (shallow average depth, large surface area, strong wind regime, and high evaporation rates), the higher hydrogen isotope signatures of the sedimentary

465   *n*-alkanes in the lake probably resulted from a dominant contribution of lakeshore vegetation.

4.3   Transport of sedimentary organic matter in the Mkhuze Wetland System

Characterization of organic matter in surface soils and sediments in terms of its stability, degree of decomposition and source vegetation, as well as their hydrological conditions in the sub-environments of the Mkhuze Wetland System, allows us to evaluate transport pathways. Plant-wax lipids are hydrophobic and associated with the mineral component of sediments (Hedges

470   and Keil, 1995; Keil et al., 1997; Wiesenberg et al., 2010). Thus, the transport and identification of sources and sinks is not exclusive to the organic component of the sediment.

In the Mkhuze Wetland System, sedimentary organic matter derived from the Mkhuze River catchment (hinterland) is deposited primarily on the floodplain, but also reaches the Mkhuze Swamps. Under present conditions, Lake St. Lucia does not receive significant quantities of sedimentary material from the hinterland nor material exported from the Mkhuze Swamps.

475   Cores retrieved from Lake St. Lucia (Benallack et al., 2016) and the Mkhuze River bayhead delta (Humphries et al., 2020) indicate that sedimentary infilling commenced 6000 - 7000 years ago when the main oceanic inlets at Lake St. Lucia sealed in response to rising sea levels during the Holocene transgression. This deposited sediment gave rise to the establishment of the current Mkhuze Swamps which currently act as an effective trap preventing the rapid siltation of the lake. An exception might be large disruptive events (severe droughts or strong floods) which occur occasionally and could induce erosion of the swamp

480   or bypassing of its filter capacity.

The high concentration of plant waxes in the upper reach of the Mkhuze River is due to low flow conditions during the sampling campaign. During the spring season, the river typically has low or even no flow (McCarthy and Hancox, 2000), resulting in the deposition of suspended sediment in the riverbed. The upper reach samples collected in this study thus likely reflect the "undiluted" hinterland signal (highly degraded, stable, C_3 woody). During periods of high flow, transported fluvial

485 OM is deposited along the river channel and on the floodplain by bank overtopping (Neal, 2001; Ellery et al., 2011). The even greater stability of the organic matter in the floodplain illustrates this depositional process (Figure 6 B). Proportions of the organic matter found in the Mkhuze Swamps are characteristically similar to that of the floodplain, so we assume that some suspended material is transported into and deposited in this sub-environment. This is clearly shown in the R- vs. I-index diagram (Figure 7), which shows several clusters of samples: (i) high R-index, low I-index (upper reach, floodplain, swamp subset), (ii)

490 low R-index, medium I-index (swamp subset), and (iii) low R-index, high I-index (lake and delta samples). Surface sedimentary OM from the delta and, in particular, the lake is significantly different from the upstream sub-environments. As discussed in the previous section, Lake St. Lucia not only experiences a significantly lower input of sedimentary organic matter and plant waxes, the deposited material does also not originate from the upstream sub-environments through which the Mkhuze River flows, but most likely from shoreline vegetation around the lake. Therefore, it can be concluded that the material transported

495 by the Mkhuze River is ultimately captured in the swamp, at least under current climatic and environmental conditions.

4.4 Local ecological implications

The identification of the Mkhuze Swamps as the ultimate sink for suspended OM from the Mkhuze River confirms previous studies that the Mkhuze Wetland System, specifically the floodplain and swamp, acts as an efficient filter upstream of Lake St. Lucia (Taylor, 1982b; Stormanns, 1987). The current active filtering and trapping function of high sediment loads, including

500 organic sedimentary organic load from the Mkhuze River, may prevent the otherwise rapid siltation of Lake St. Lucia.

OM in the surface sediments of Lake St. Lucia originates primarily from lakeshore vegetation, as indicated by the lake transect data shown in comparison with upstream areas of the system. However, some studies (Taylor, 1982b) assume that the Mkhuze Swamps, in their function as freshwater reservoirs ("sponges") (Alexander, 1973), are also responsible for input of OM, serving as a potential energy source in Lake St. Lucia. Our data on particulate organic matter contradict this assumption

505 showing that sedimentary particulate OM is presently not transported from the hinterland nor exported directly from the swamp.

In contrast, OM export from wetlands occurs primarily through the export of dissolved organic matter (DOC, Cole et al., 2007), which accounts for about 90 % of total OM (Reddy and DeLaune, 2008). In saline waters, like Lake St. Lucia, DOM is likely to flocculate (Ardón et al., 2016). Assuming that OM is exported in dissolved form from the Mkhuze Swamps, it should thus be detectable in the lake transect surface samples, but this was not observed in this study. In part, this could be due to

510 the fact that a significant porportion of DOC may be removed by sorption onto precipitating oxides when sediments contain substantial amounts of aluminum and iron metal oxides (McKnight et al., 1992), as is the case in upstream sub-environments. With the employed methods we cannot confirm neither any particulate OC nor DOC export from the Mkhuze Wetland System into Lake St. Lucia.

The present study is the first examining sedimentary OM transport within the Mkhuze Wetland System, revealing that OM is indeed transported even to the Mkhuze Swampsand not being just deposited near the river channel and on the floodplain. Three processes might play a role for transport of material into the swamps: (i) the ongoing eastward progression of the floodplain (McCarthy and Hancox, 2000), (ii) transport during severe flood events caused by cyclones and cutoff lows , or (iii) that channelization has had an impact on the transport efficiency. The transport path of the Mkhuze River has been dramatically shortened by channelization (see section 2.1.3). As a result, most of the Mkhuze River water now flows through the Tshanetshe-Demazane Canal System (Stormanns, 1987; Neal, 2001; Barnes et al., 2002; Ellery et al., 2003), which may have altered sediment transport. A shift in the area of deposition of material transported by the Mkhuze River is likely to affect the local vegetation distribution, i.e. causing a shift in the ecological zones by altered substrate conditions. In general, however, the Mkhuze Wetland System overall appears to exhibit high resilience against natural and/or anthropogenic induced changes. The severe drought of 2016, which led to the drying of large parts of Lake St. Lucia, does not seem to have had any lasting impact on the filtering function of the swamps. Likewise, the establishment of the canal system also does not appear to have caused lasting damage to the filtering function of the Mkhuze Swamps.

4.5   Fate of sedimentary organic matter in wetlands

In comparison with humid region (tropical and temperate) wetlands, the Mkhuze Wetland System exhibits distinctive characteristics that reflect the low ratio between precipitation and potential evapotranspiration characterizing the region (Figure 2). High evaporative demand and transmission losses from the river to the surrounding floodplain, result in marked declines in both channel width and depth downstream (Humphries et al., 2010). Downstream decreases in discharge and stream power result in a gradual decline in ability of the Mkhuze River to transport particulate material, ultimately terminating in the Mkhuze swamps. Although typically unusual, such downstream changes appear to be distinctive features of wetlands found in sub-humid and semi-arid regions of the world (Tooth and McCarthy, 2007), and is likely an important reason why the Mkhuze Wetland System acts as such an efficient trap for organic material.

Most large tropical and temperate river systems are associated with wetlands (Wetzel, 2001; Ward et al., 2017) along their river courses. For example, studies conducted on the Cuvette Congolaise (Runge, 2007), a large wetland system traversed by the Congo River, indicate that fluvially transported particulate OM signals from upstream sources are seasonally overprinted by storage and release of particulates in and from the wetlands (Hemingway et al., 2016, 2017). Depending on variable climatic conditions throughout the year, the Cuvette Congolaise wetlands may thus show a similar trapping function of transported material than the Mkhuze Wetland System under relatively dry conditions while showing increased export from material at higher water flows (Hemingway et al., 2017). Wetlands may thus switch from a trapping function to export of carbon depending on hydrological conditions and seasonal climatic changes.

This differential trapping and export functions of wetlands need to be considered when reconstructing climatic changes based on sedimentary archives recovered from terminal lakes and offshore archives. Depending on the activity and efficiency of wetlands, material from more upstream areas will effectively masked by wetlands depending on their hydrologic state and can even be overprinted be wetland export of OM or OM input from downstream areas. Such a process has been suggested

for the transport of OM in the Amazon River system, where Andean material is effectively overprinted by lowland sources from rainforests, floodplains and wetlands (Quay et al., 1992; Blair et al., 2004). In such cases, reconstructing environmental

550 changes in the integrated watershed using offshore archives may thus not be possible. Wetland systems with an active trapping function effectively change the transported OM, so that signals detected in offshore archives instead reflect specific sections of the river catchment. Other sediment related proxies may also be affected by wetland trapping, so such geomorphological settings could have a much stronger influence than is often assumed. Combining environmental analyses with specific markers released from wetlands, on the other hand, allows an assessment of the hydrologic changes that lead to inefficient OM trapping

555 and degradation of wetlands (e.g., Schefuß et al., 2016).

In addition, carbon sequestration and the ability of wetlands to act as carbon sinks are considered to play an important role in the global carbon budget. There is concern that global warming may alter the hydrological balance of wetlands, releasing significant amounts of carbon to the atmosphere through direct oxidation processes or to adjacent water bodies through erosion of wetland soils, as has been observed for the Cuvette Congolaise and elsewhere (Hemingway et al., 2017). In certain cases,

560 extreme weather events, which are expected to become more frequent as the global climate changes, have also been shown to promote the release of DOC from wetlands (Rudolph et al., 2020). It is likely that particulate material would also be exported by excessive flooding, as is similarly observed by increased flushing of terrestrial carbon into river systems (Bianchi et al., 2013). Thus, the trapping function of wetlands, overridden by overloading, would just as likely contribute to increased carbon dioxide emissions to the atmosphere through turnover of exported OM in adjacent waters.

565 5 Conclusions

We present a spatial assessment of TOC concentrations, OM composition (δ^{13}C, C/N, HI, R-index, I-index), n-alkane distributions, and their respective compound-specific stable carbon (δ^{13}C$_{n-alkane}$) and hydrogen (δD$_{n-alkane}$) isotope compositions along an approx. 130 km-long transect of the Mkhuze River and plant wax data from locally dominant plant species to constrain the origin and transport pathways of OM through and within the sub-environments of the Mkhuze Wetland System,

570 South Africa. Our results indicate that degraded OM originating from the hinterland is deposited primarily on the floodplain of the Mkhuze River and partially in the downstream swamp. The Mkhuze Swamps currently efficiently trap OM under low flow conditions, so neither release hinterland material nor export swamp-derived OM to Lake St. Lucia (Figure 10).

The surface sediments in the upper reach show allochthonous inputs from the Mkhuze River basin. OM concentrations are low and show a degraded signature associated with a C$_3$ woody source vegetation, which experienced relatively dry growing

575 conditions. Sedimentary OM in the floodplain and swamp exhibit high variability in their source signatures and degradation status reflecting environmental diversity, with samples from the floodplain characterized by a mixture of degraded OM from the hinterland and fresh OM. The most pronounced C$_4$ signatures are encountered, attributed to agricultural use of the floodplain. OM from surface samples in the Mkhuze Swamps also shows a degraded signature but reflects increasing inputs of local wetland sedges and wetland grasses. In contrast, OM from Lake St. Lucia shows completely different characteristics, such as
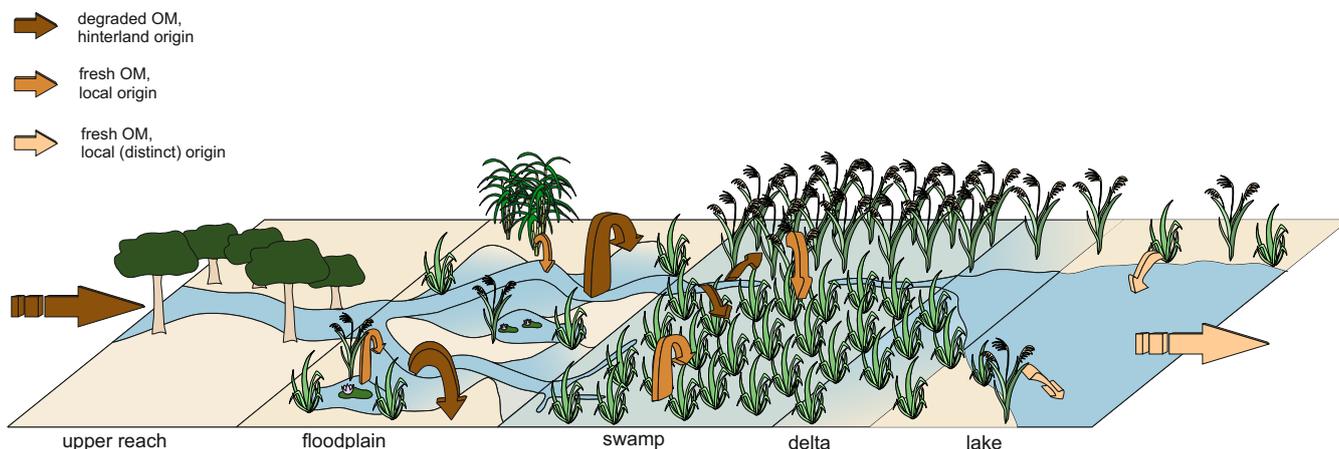
Figure 10. The figure shows a schematic summary of the characteristics and transport pathways of organic material in a terminal or flow-through wetland system under low flow conditions. The vegetation types shown (trees, wetland sedges, grasses, and aquatic species) indicate the prominently occurring vegetation in each sub-environment of the Mkhuze Wetland System. Arrows indicate OM input and deposition, with thickness of arrows corresponding to OM quantity assumption and colours corresponding to OM quality characteristics (dark brown: more degraded, light brown: less degraded, spatially different origin).

580 much lower concentrations and much less degradation due to proximal terrestrial inputs rather than aquatic contributions. Plant wax data confirms these findings, pointing to lake shoreline vegetation as the main source.

This study shows that traversed or terminal wetlands under certain conditions, such as low flow, in this case a result of climatic factors, i.e., evaporation exceeds precipitation, can capture OM so efficiently that transport from upstream areas does not occur and downstream OM originates almost exclusively from the immediate vicinity.

585 We emphasize that such wetlands, as geomorphological features within river systems, can impact environmental studies based on terminal sediments, thereby assuming watershed-integrated information. In addition, disturbances, e.g., by extreme weather events, which are assumed to become more frequent under global climate change, are likely to affect the trapping function of wetlands and thus increase export of previously stored OM, leading to an increase in carbon emissions through turnover of exported OM in adjacent waterbodies.

590 *Code and data availability.* The research data has been submitted to Pangaea, but a DOI is not yet assigned.

References

Albrecht, R., Sebag, D., and Verrecchia, E.: Organic matter decomposition: bridging the gap between Rock–Eval pyrolysis and chemical

610 characterization (CPMAS13C NMR), Biogeochemistry, 122, 101–111, https://doi.org/10.1007/s10533-014-0033-8, 2015.

Alexander, W. J. R.: Some comment on the diversion of the Mkuze river in Lake St. Lucia, Tech. rep., 1973.

Alexander, W. J. R., Stormanns, C., and Breen, C.: Some aspects of the hydrology of the Mkuze Swamp system, in: Proceedings of the
Greater Mkuze Swamp System Symposium and Workshop, Institute of Natural Resources, Pietermaritzburg, pp. 4–7, 1986.

Ardón, M., Helton, A. M., and Bernhardt, E. S.: Drought and saltwater incursion synergistically reduce dissolved organic carbon export from

615 coastal freshwater wetlands, Biogeochemistry, 127, 411–426, 2016.

Baas, M., Pancost, R., Van Geel, B., and Sinninghe Damsté, J. S.: A comparative study of lipids in Sphagnum species, Organic Geochemistry,
31, 535–541, https://doi.org/10.1016/S0146-6380(00)00037-1, 2000.

Badewien, T., Vogts, A., and Rullkötter, J.: n-Alkane distribution and carbon stable isotope composition in leaf waxes of C3 and C4 plants
from Angola, Organic Geochemistry, 89-90, 71–79, https://doi.org/https://doi.org/10.1016/j.orggeochem.2015.09.002, 2015.

620 Barnes, K., Ellery, W. N., and Kindness, A.: A preliminary analysis of water chemistry of the Mkuze Wetland System, KwaZulu-Natal: A
mass balance approach, Water SA, 28, 1–12, https://doi.org/10.4314/wsa.v28i1.4861, 2002.

Behar, F., Beaumont, V., and Penteado, H. L. D. B.: Rock-Eval 6 technology: performances and developments, Oil & Gas Science and
Technology, 56, 111–134, 2001.

Benallack, K., Green, A. N., Humphries, M. S., Cooper, J. A., Dladla, N. N., and Finch, J. M.: The stratigraphic evolution of a large back-

625 barrier lagoon system with a non-migrating barrier, Marine Geology, 379, 64–77, https://doi.org/10.1016/j.margeo.2016.05.001, 2016.

Bianchi, T. S., Garcia-Tigreros, F., Yvon-Lewis, S. A., Shields, M., Mills, H. J., Butman, D., Osburn, C., Raymond, P., Shank, G. C., DiMarco,
S. F., Walker, N., Reese, B. K., Mullins-Perry, R., Quigg, A., Aiken, G. R., and Grossman, E. L.: Enhanced transfer of terrestrially derived
carbon to the atmosphere in a flooding event, Geophysical Research Letters, 40, 116–122, https://doi.org/10.1029/2012GL054145, 2013.

Blair, N. E., Leithold, E. L., and Aller, R. C.: From bedrock to burial: The evolution of particulate organic carbon across coupled watershed-

630 continental margin systems, Marine Chemistry, 92, 141–156, https://doi.org/10.1016/j.marchem.2004.06.023, 2004.

Bush, R. T. and McInerney, F. A.: Leaf wax n-alkane distributions in and across modern plants: Implications for paleoecology and chemo-
taxonomy, Geochimica et Cosmochimica Acta, 117, 161–179, https://doi.org/10.1016/j.gca.2013.04.016, 2013.

Carr, A. S., Boom, A., Grimes, H. L., Chase, B. M., Meadows, M. E., and Harris, A.: Leaf wax n-alkane distributions in arid zone
South African flora: Environmental controls, chemotaxonomy and palaeoecological implications, Organic Geochemistry, 67, 72–84,

635 https://doi.org/https://doi.org/10.1016/j.orggeochem.2013.12.004, 2014.

Cole, J. J., Prairie, Y. T., Caraco, N. F., McDowell, W. H., Tranvik, L. J., Striegl, R. G., Duarte, C. M., Kortelainen, P., Downing, J. A., Mid-
delburg, J. J., and Melack, J.: Plumbing the global carbon cycle: Integrating inland waters into the terrestrial carbon budget, Ecosystems,
10, 171–184, https://doi.org/10.1007/s10021-006-9013-8, 2007.

Collister, J. W., Rieley, G., Stern, B., Eglinton, G., and Fry, B.: Compound-specific δ 13C analyses of leaf lipids from plants with differing

640 carbon dioxide metabolisms, Organic Geochemistry, 21, 619–627, https://doi.org/10.1016/0146-6380(94)90008-6, 1994.

Cooper, J. E. and Bray, E. E.: A postulated role of fatty acids in petroleum formation, Geochimica et Cosmochimica Acta, 27, 1113–1127,
1963.

Diefendorf, A. F. and Freimuth, E. J.: Extracting the most from terrestrial plant-derived n-alkyl lipids and their carbon isotopes from the
sedimentary record: A review, Organic Geochemistry, 103, 1–21, 2017.

645   Disnar, J. R., Guillet, B., Keravis, D., Di-Giovanni, C., and Sebag, D.: Soil organic matter (SOM) characterization by Rock-Eval pyrolysis:
Scope and limitations, Organic Geochemistry, 34, 327–343, https://doi.org/10.1016/S0146-6380(02)00239-5, 2003.

Ellery, W. N., Dahlberg, A. C., Strydom, R., Neal, M. J., and Jackson, J.: Diversion of water flow from a floodplain wetland stream: an
analysis of geomorphological setting and hydrological and ecological consequences, Journal of Environmental Management, 68, 51–71,
2003.

650   Ellery, W. N., Grenfell, S. E., Grenfell, M. C., Humphries, M. S., and Barnes, K. B.: The wetlands, in: Ecology and Conserva-
tion of Estuarine Ecosystems: Lake St Lucia as a Global Model, May 2019, chap. 6, pp. 95–112, Cambridge University Press,
https://doi.org/10.1017/CBO9781139095723.008, 2011.

Espitalie, J., Deroo, G., and Marquis, F.: Rock-Eval pyrolysis and its applications (part one), Oil & Gas Science and Technology-Revue
d'IFPEN, 40, 563–579, 1985.

655   Ficken, K. J., Li, B., Swain, D. L., and Eglinton, G.: An n-alkane proxy for the sedimentary input of submerged/floating freshwater aquatic
macrophytes, Organic Geochemistry, 31, 745–749, 2000.

Hedges, J. I. and Keil, R. G.: Sedimentary organic matter preservation: an assessment and speculative synthesis-a comment, Marine Chem-
istry, 49, 81–115, https://doi.org/10.1016/0304-4203(95)00011-F, 1995.

Hemingway, J. D., Schefuß, E., Dinga, B. J., Pryer, H., and Galy, V. V.: Multiple plant-wax compounds record differential sources and
660   ecosystem structure in large river catchments, Geochimica et Cosmochimica Acta, 184, 20–40, https://doi.org/10.1016/j.gca.2016.04.003,
2016.

Hemingway, J. D., Schefuß, E., Spencer, R. G., Dinga, B. J., Eglinton, T. I., McIntyre, C., and Galy, V. V.: Hydrologic controls on sea-
sonal and inter-annual variability of Congo River particulate organic matter source and reservoir age, Chemical Geology, 466, 454–465,
https://doi.org/10.1016/j.chemgeo.2017.06.034, 2017.

665   Hemond, H. F. and Benoit, J.: Cumulative Impacts o n Water Quality Functions of Wetlands, Environmental Management, 12, 639–653,
1988.

Holm, L. G., Plucknett, D. L., Pancho, J. V., and Herberger, J. P.: The world's worst weeds. Distribution and biology., University press of
Hawaii, 1977.

Humphries, M., Green, A., Higgs, C., Strachan, K., Hahn, A., Pillay, L., and Zabel, M.: High-resolution geochemical
670   records of extreme drought in southeastern Africa during the past 7000 years, Quaternary Science Reviews, 236, 106 294,
https://doi.org/10.1016/j.quascirev.2020.106294, 2020.

Humphries, M. S., Kindness, A., Ellery, W. N., Hughes, J. C., and Benitez-Nelson, C. R.: 137Cs and 210Pb derived sediment accumu-
lation rates and their role in the long-term development of the Mkuze River floodplain, South Africa, Geomorphology, 119, 88–96,
https://doi.org/10.1016/j.geomorph.2010.03.003, 2010.

675   Hutchison, I. P. G.: The hydrology of the St Lucia system, in: St Lucia scientific advisory council workshop meeting at Charters Creek, pp.
15–17, 1976.

Hutchison, I. P. G. and Pitman, W. V.: St. Lucia Lake Research Report. Volume 1: Climatology and hydrology of the St. Lucia Lake system,
Tech. rep., 1973.

Johnston, C. A.: Sediment and nutrient retention by freshwater wetlands: Effects on surface water quality, Critical Reviews in Environmental
680   Control, 21, 491–565, https://doi.org/10.1080/10643389109388425, 1991.

Junk, W. J. and An, S.: Current state of knowledge regarding the world ' s wetlands and their future under global climate change : a synthesis,
Aquatic sciences, pp. 151–167, https://doi.org/10.1007/s00027-012-0278-z, 2013.

Keil, R. G., Mayer, L. M., Quay, P. D., Richey, J. E., and Hedges, J. I.: Loss of organic matter from riverine particles in deltas, Geochimica et Cosmochimica Acta, 61, 1507–1511, https://doi.org/10.1016/S0016-7037(97)00044-6, 1997.

685   Lafargue, E., Marquis, F., and Pillot, D.: Rock-Eval 6 applications in hydrocarbon exploration, production, and soil contamination studies, Revue de l'institut français du pétrole, 53, 421–437, 1998.

Liu, H., Liu, Z., Zhao, C., and Liu, W.: n-Alkyl lipid concentrations and distributions in aquatic plants and their individual δD variations, Science China Earth Sciences, 62, 1441–1452, 2019.

Liu, J., An, Z., and Liu, H.: Leaf wax n-alkane distributions across plant types in the central Chinese Loess Plateau, Organic Geochemistry,
690   125, 260–269, https://doi.org/https://doi.org/10.1016/j.orggeochem.2018.09.006, 2018.

Malou, O. P., Sebag, D., Moulin, P., Chevallier, T., Badiane-Ndour, N. Y., Thiam, A., and Chapuis-Lardy, L.: The Rock-Eval® signature of soil organic carbon in arenosols of the Senegalese groundnut basin. How do agricultural practices matter?, Agriculture, Ecosystems & Environment, 301, 107 030, 2020.

Maud, R. R.: The climate and geology of Maputaland, Studies on the Ecology of Maputaland, pp. 1–7, 1980.

695   McCarthy, T. S. and Hancox, P. J.: Wetlands, in: The Cenozoic of Southern Africa, Oxford University Press, New York, 2000.

McKnight, D. M., Bencala, K. E., Zellweger, G. W., Aiken, G. R., Feder, G. L., and Thorn, K. A.: Sorption of dissolved organic carbon by hydrous aluminum and iron oxides occurring at the confluence of Deer Creek with the Snake River, Summit County, Colorado, Environmental science & technology, 26, 1388–1396, 1992.

Mitsch, W. J. and Gosselink, J. G.: Wetlands (5th edition), John Wiley \& Sons, https://doi.org/10.1108/rr-09-2015-0230, 2015.

700   Neal, M. J.: The vegetation ecology of the lower Mkuze river floodplain, Northern KwaZulu-Natal: a landscape ecology perspective., Ph.D. thesis, University of Natal-Durban, 2001.

Perissinotto, R., Stretch, D. D., and Taylor, R. H.: Ecology and conservation of estuarine ecosystems: Lake St Lucia as a global model, Cambridge University Press, 2013.

Pillot, D., Deville, E., and Prinzhofer, A.: Identification and quantification of carbonate species using Rock-Eval pyrolysis, Oil & Gas Science
705   and Technology–Revue d'IFP Energies nouvelles, 69, 341–349, 2014.

Porter, R. N.: South Africa's first world heritage site, in: Ecology and Conservation of Estuarine Ecosystems: Lake St Lucia as a Global Model. Cambridge University Press, New York, chap. 1, pp. 1–21, Cambridge University Press, 2013.

Poynter, J. and Eglinton, G.: 14. Molecular composition of three sediments from hole 717c: The Bengal fan, in: Proceedings of the Ocean Drilling Program: Scientific results, vol. 116, pp. 155–161, 1990.

710   Quay, P. D., Wilbur, D. ., Richey, J. E., Hedges, J. I., Devol, A. H., and Victoria, R.: Carbon cycling in the Amazon River: Implications from the 13C compositions of particles and solutes, Limnology and Oceanography, 37, 857–871, https://doi.org/10.4319/lo.1992.37.4.0857, 1992.

Reddy, K. R. and Debusk, T. A.: State-of-the-art utilization of aquatic plants in water pollution control, Water science and technology, pp. 61–79, 1987.

715   Reddy, K. R. and DeLaune, R. D.: Biogeochemistry of wetlands: science and applications, CRC press, 2008.

Reuter, H., Gensel, J., Elvert, M., and Zak, D.: Evidence for preferential protein depolymerization in wetland soils in response to external nitrogen availability provided by a novel FTIR routine, Biogeosciences, 17, 499–514, https://doi.org/10.5194/bg-17-499-2020, 2020.

Rommerskirchen, F., Plader, A., Eglinton, G., Chikaraishi, Y., and Rullkötter, J.: Chemotaxonomic significance of distribution and stable carbon isotopic composition of long-chain alkanes and alkan-1-ols in C4 grass waxes, Organic Geochemistry, 37, 1303–1332,
720   https://doi.org/10.1016/j.orggeochem.2005.12.013, 2006.

Biogeosciences
Discussions
Open Access
EGU

Rudolph, J. C., Arendt, C. A., Hounshell, A. G., Paerl, H. W., and Osburn, C. L.: Use of Geospatial, Hydrologic, and Geochemical Modeling to Determine the Influence of Wetland-Derived Organic Matter in Coastal Waters in Response to Extreme Weather Events, Frontiers in Marine Science, 7, 1–18, https://doi.org/10.3389/fmars.2020.00018, 2020.

Runge, J.: The Congo River, Central Africa, Large rivers: geomorphology and management, pp. 293–309, 2007.

725 Sachse, D., Billault, I., Bowen, G. J., Chikaraishi, Y., Dawson, T. E., Feakins, S. J., Freeman, K. H., Magill, C. R., McInerney, F. A., and Van Der Meer, M. T. J.: Molecular paleohydrology: interpreting the hydrogen-isotopic composition of lipid biomarkers from photosynthesizing organisms, Annual Review of Earth and Planetary Sciences, 40, 221–249, 2012.

Schefuß, E., Eglinton, T. I., Spencer-Jones, C. L., Rullkötter, J., De Pol-Holz, R., Talbot, H. M., Grootes, P. M., and Schneider, R. R.: Hydrologic control of carbon cycling and aged carbon discharge in the Congo River basin, Nature Geoscience, 9, 687–690,
730 https://doi.org/10.1038/ngeo2778, 2016.

Sebag, D., Verrecchia, E. P., Cécillon, L., Adatte, T., Albrecht, R., Aubert, M., Bureau, F., Cailleau, G., Copard, Y., Decaens, T., Disnar, J. R., Hetényi, M., Nyilas, T., and Trombino, L.: Dynamics of soil organic matter based on new Rock-Eval indices, Geoderma, 284, 185–203, https://doi.org/10.1016/j.geoderma.2016.08.025, 2016.

Sebag, D., Garcin, Y., Adatte, T., Deschamps, P., Ménot, G., and Verrecchia, E. P.: Correction for the siderite effect on Rock-Eval parameters:
735 application to the sediments of Lake Barombi (southwest Cameroon), Organic Geochemistry, 123, 126–135, 2018.

Sessions, A. L.: Factors controlling the deuterium contents of sedimentary hydrocarbons, Organic Geochemistry, 96, 43–64, 2016.

Stormanns, C.: An inventory and assessment of the conservation value of the Mkuze Swamp System, National Conservation Resources, CSIR, Pretoria, 1987.

Taylor, R., Kelbe, B., Haldorsen, S., Botha, G. A., Wejden, B., Väret, L., and Simonsen, M. B.: Groundwater-dependent ecology of the
740 shoreline of the subtropical Lake St Lucia estuary, Environmental Geology, pp. 586–600, https://doi.org/10.1007/s00254-005-0095-y, 2006.

Taylor, R. H.: St Lucia Estuary: the aquatic environment, the physical and chemical characteristics, St Lucia Research Review, pp. 42–56, 1982a.

Taylor, R. H.: The Mkuze Swamps, St Lucia Research Review, pp. 201–210, 1982b.

745 Taylor, R. H.: The past and present human involvement in the Mkuze swamp system, in: Proceedings of the greater Mkuze swamp system symposium and workshop, Institute of Natural Resources, Report, 22, 1986.

Taylor, R. H.: Management history, in: Ecology and conservation of estuarine ecosystems: Lake St Lucia as a global model, May 2019, chap. 2, Cambridge University Press, 2013.

Tinley, K.: a preliminary report on the ecology of the Pongola and Mkuze flood plains, 1959.

750 Tooth, S. and McCarthy, T. S.: Wetlands in drylands: geomorphological and sedimentological characteristics, with emphasis on examples from southern Africa, Progress in Physical Geography: Earth and Environment, 31, 3–41, https://doi.org/10.1177/0309133307073879, 2007.

Van Heerden, I. L. and Swart, D. H.: St. Lucia Research: An assessment of past and present geomorphological and sedimentary processes operative in the St. Lucia Estuary and environs, vol. 569, Marine Geoscience and Sediment Dynamics Divisions, National Research . . . ,
755 1986.

Vogts, A., Moossen, H., Rommerskirchen, F., and Rullkötter, J.: Distribution patterns and stable carbon isotopic composition of alkanes and alkan-1-ols from plant waxes of African rain forest and savanna C3 species, Organic Geochemistry, 40, 1037–1054, https://doi.org/10.1016/j.orggeochem.2009.07.011, 2009.

Vogts, A., Schefuß, E., Badewien, T., and Rullkötter, J.: n-Alkane parameters from a deep sea sediment transect off southwest Africa reflect
760   continental vegetation and climate conditions, Organic Geochemistry, 47, 109–119, https://doi.org/10.1016/j.orggeochem.2012.03.011,
       2012.

Ward, N. D., Bianchi, T. S., Medeiros, P. M., Seidel, M., Richey, J. E., Keil, R. G., and Sawakuchi, H. O.: Where Carbon Goes When Water
       Flows: Carbon Cycling across the Aquatic Continuum, Frontiers in Marine Science, 4, 1–27, https://doi.org/10.3389/fmars.2017.00007,
       2017.

765   Watkeys, M. K., Mason, T. R., and Goodman, P. S.: The rôle of geology in the development of Maputaland, South Africa, Journal of African
       Earth Sciences, 16, 205–221, https://doi.org/10.1016/0899-5362(93)90168-P, 1993.

Wetzel, R. G.: Limnology: lake and river ecosystems, gulf professional publishing, https://doi.org/10.1063/1.3224729, 2001.

Whitfield, A. K. and Taylor, R. H.: A review of the importance of freshwater inflow to the future conservation of Lake St Lucia, Aquatic
       Conservation: Marine and Freshwater Ecosystems, 19, 838–848, 2009.

770   Wiesenberg, G. L., Dorodnikov, M., and Kuzyakov, Y.: Source determination of lipids in bulk soil and soil density fractions after four years
       of wheat cropping, Geoderma, 156, 267–277, https://doi.org/10.1016/j.geoderma.2010.02.026, 2010.